Gene Cheung
Associate Professor, York University
26th September, 2018

Graph Spectral Image Processing

.

Acknowledgement

Collaborators:

- Y. Nakatsukasa (NII, Japan)
- S. Muramatsu (Niigata, Japan)
- **A. Ortega** (USC, USA)
- **D. Florencio** (MSR, USA)
- **P. Frossard** (EPFL, Switzerland)
- J. Liang, I. Bajic (SFU, Canada)
- X. Wu (McMaster U, Canada)
- V. Stankovic (U of Strathclyde, UK)
- **P. Le Callet** (U of Nantes, France)
- **X. Liu** (HIT, China)
- W. Hu, J. Liu, Z. Guo, W. Gao (Peking U., China)
- X. Ji, L. Fang (Tsinghua, China)
- Y. Zhao (BJTU, China)
- **C.-W. Lin** (National Tsing Hua University, Taiwan)
- E. Peixoto, B. Macchiavello, E. M. Hung (U. Brasilia, Brazil)







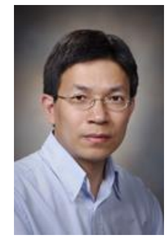



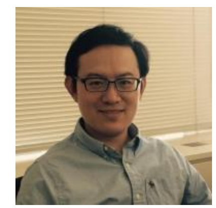

YORK UNIVERSITÉ UNIVERSITY

VISION: SCIENCE TO APPLICATIONS (VISTA)

www.yorku.ca/vista

CANADA FIRST RESEARCH EXCELLENCE FUND | APOGÉE CANADA FONDS D'EXCELLENCE EN RECHERCHE

Vision: Science to Applications Program

Funded by: Canada First Research Excellence Fund

- VISTA's Mission: to support transdisciplinary vision research, bridging fundamental and applied vision research, both computational and biological.
- VISTA involves CVR and 5 other York research groups, 5 Faculties, 49 investigators (so far), and over 50 partners (hospitals, industry, international research groups, etc.)
- VISTA funds new faculty positions, research chairs, staff, post-doctoral fellows, graduate students, research grants, travel scholarships and commercialization.
- Federal funding of $33.34M; partners bring total to $120M.
- For more info, see:

http://vista.info.yorku.ca/

CANADA FIRST RESEARCH EXCELLENCE FUND | APOGÉE CANADA FONDS D'EXCELLENCE EN RECHERCHE

VISTA Research Concept

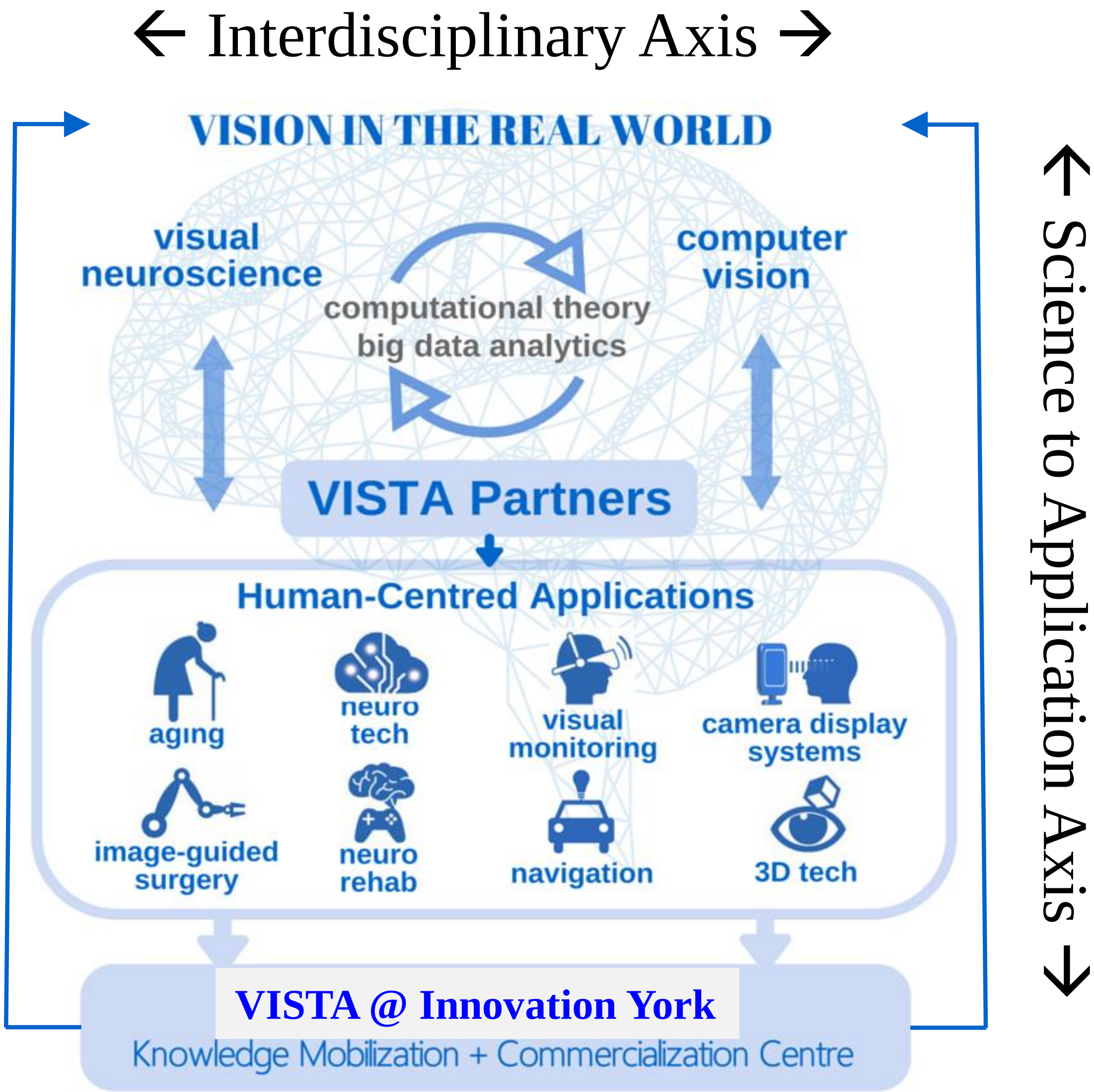

Opportunities for International Collaboration

Opportunity	Description	Amount
Research Grants	Partner-based research projects	$50,000 per project
Travel Awards	Travel/accommodations for faculty and trainees to undertake collaborative research with partner institutions	$7,500-$10,000 per visit
Prototyping Funds	Development of prototypes for York researchers in the vision sciences	$50,000 per project
Graduate Scholarships	Salary stipends for Masters and PhD students above other external or internal funds	$10,000 per year
Postdoctoral Fellowships	Salary plus research allowance and travel funds over a 2-year period	$55,000-$70,000 per year + $8,500 per year

For more information: yorku.ca/vista

YORK UNIVERSITÉ UNIVERSITY

VISTA Contacts

- Doug Crawford, Scientific Director
  - jdc@yorku.ca
- Richard Wildes, Associate Director
  - wildes@cse.yorku.ca
- Jennifer Teague, Program Manager
  - jteague@yorku.ca

Outline

- GSP Fundamentals
- GSP for Image Compression
  - Optimality of GFT
- GSP for Inverse Imaging
  - Graph Laplacian Regularizer
  - Reweighted Graph TV
- Deep GLR
- Ongoing & Future Work

Outline

- GSP Fundamentals
- GSP for Image Compression
  - Optimality of GFT
- GSP for Inverse Imaging
  - Graph Laplacian Regularizer
  - Reweighted Graph TV
- Deep GLR
- Ongoing & Future Work

Digital Signal Processing

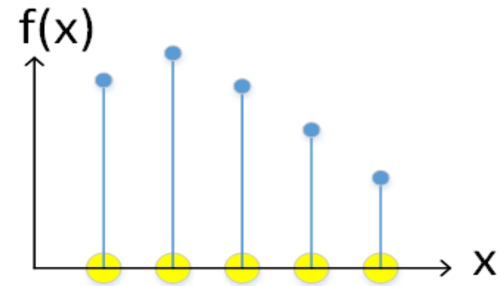

- Discrete signals on ***regular*** data kernels.
  - Ex.1: audio on regularly sampled timeline.
  - Ex.2: image on 2D grid.

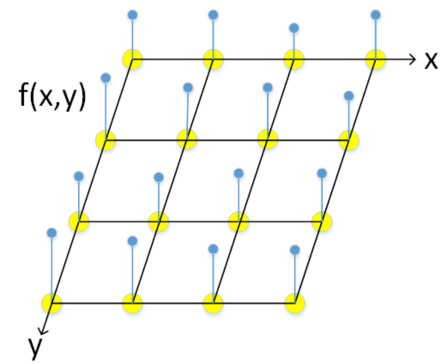

- **Harmonic analysis** tools (transforms, wavelets) for diff. tasks:
  - Compression.
  - Restoration.
  - Segmentation, classification.

Smoothness of Signals

- Signals are often **smooth**.
- Notion of *frequency*, *band-limited*.
- Ex.: **DCT**:

$$X_k = \sum_{n=0}^{N-1} x_n \cos\left(\frac{\pi}{N}\left(n+\frac{1}{2}\right)k\right)$$

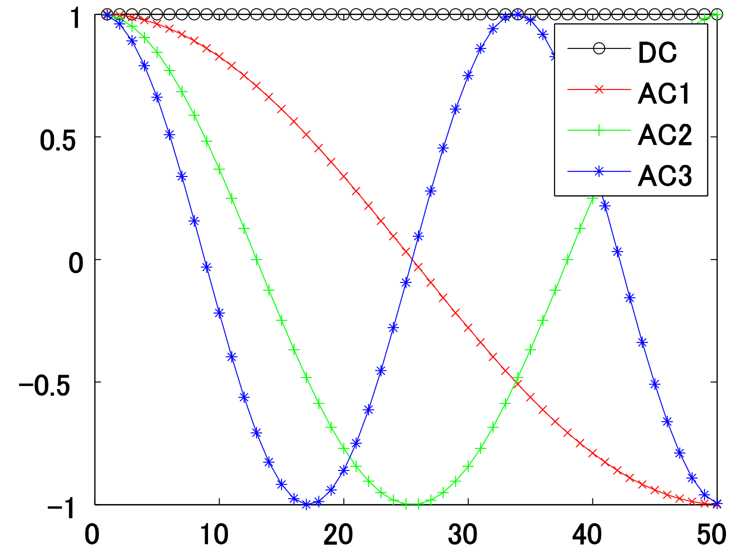

2D DCT basis

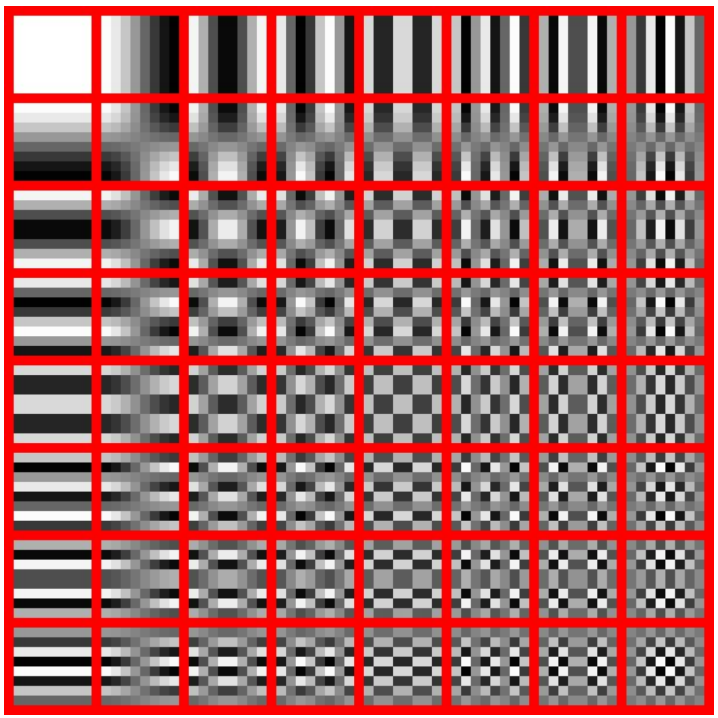

$$\mathrm{a} = \Phi\,\mathrm{x}$$

desired signal

transform

transform coeff.

$$\mathrm{a} = \begin{bmatrix} a_0 \\ a_1 \\ 0 \\ \vdots \\ 0 \end{bmatrix}$$

Compact signal representation

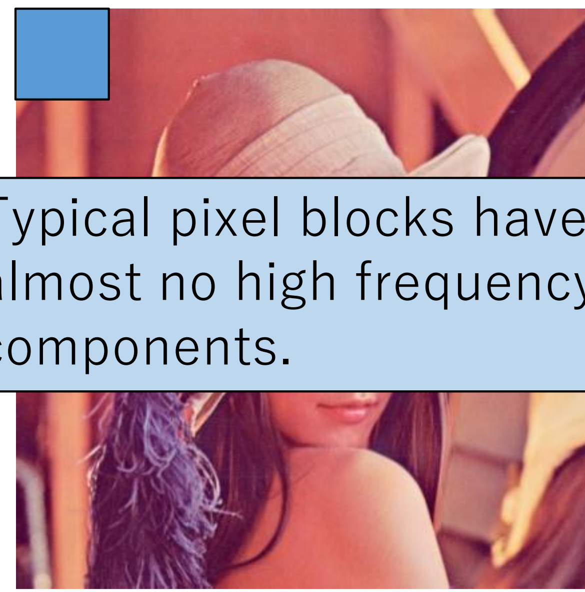

Typical pixel blocks have almost no high frequency components.

Graph Signal Processing

- Signals on ***irregular*** data kernels described by graphs.
  - Graph: nodes and edges.
  - Edges reveals *node-to-node relationships*.

1. Data domain is naturally a graph.
   - Ex: ages of users on social networks.

2. Underlying data structure unknown.
   - Ex: images: 2D grid → structured graph.

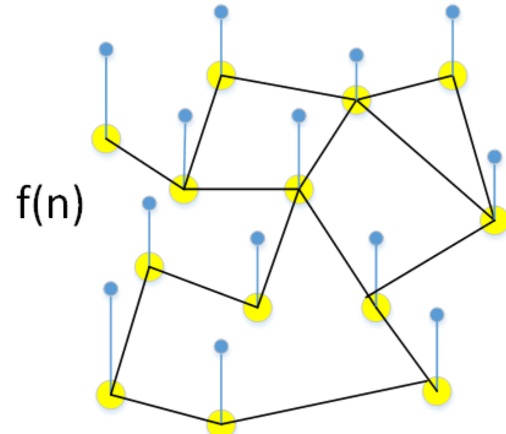

example graph-signal

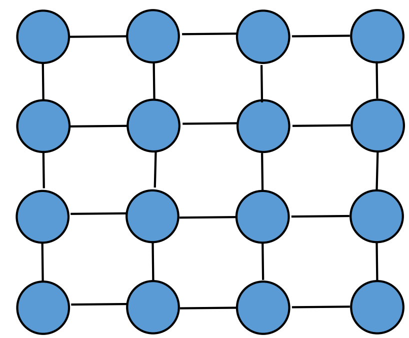

Graph Signal Processing (GSP) addresses the problem of processing signals that live on graphs.

[1] D. I. Shuman et al.,"**The Emerging Field of Signal Processing on Graphs: Extending High-dimensional Data Analysis to Networks and other Irregular Domains**," *IEEE Signal Processing Magazine*, vol.30, no.3, pp.83-98, 2013.

Graph Signal Processing

Research questions*:

- **Sampling**: how to efficiently acquire / sense a graph-signal?
  - Graph sampling theorems.
- **Representation**: Given graph-signal, how to compactly represent it?
  - Transforms, wavelets, dictionaries.
- **Signal restoration**: Given noisy and/or partial graph-signal, how to recover it?
  - Graph-signal priors.

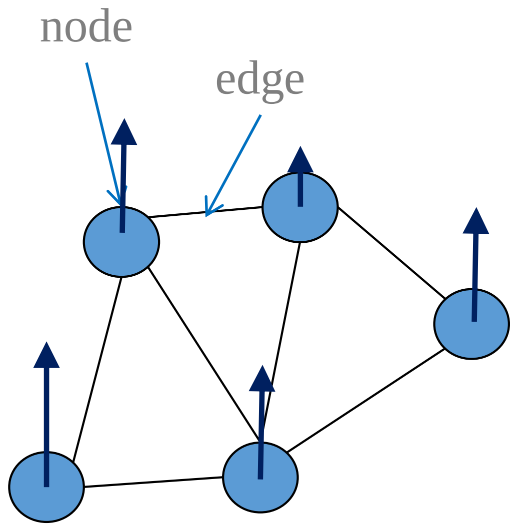

*__Graph Signal Processing Workshop__, Philadelphia, US, May, 2016. https://alliance.seas.upenn.edu/~gsp16/wiki/index.php?n=Main.Program
*__Graph Signal Processing Workshop__, Pittsburgh, US, May, 2017. https://gsp17.ece.cmu.edu/
*__Graph Signal Processing Workshop__, Lausanne, Switzerland, June, 2018. https://gsp18.epfl.ch/

Graph Fourier Transform (GFT)

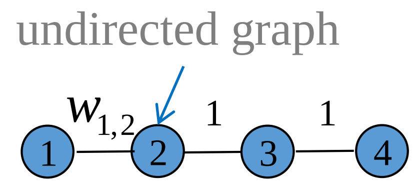

Graph Laplacian:

- *Adjacency Matrix A*: entry $A_{i,j}$ has *non-negative* edge weight $w_{i,j}$ connecting nodes i and j.

$$A = \begin{bmatrix} 0 & w_{1,2} & 0 & 0 \\ w_{1,2} & 0 & 1 & 0 \\ 0 & 1 & 0 & 1 \\ 0 & 0 & 1 & 0 \end{bmatrix}$$

- *Degree Matrix D*: diagonal matrix w/ entry $D_{i,i}$ being sum of column entries in row i of A.

$$D = \begin{bmatrix} w_{1,2} & 0 & 0 & 0 \\ 0 & w_{1,2}+1 & 0 & 0 \\ 0 & 0 & 2 & 0 \\ 0 & 0 & 0 & 1 \end{bmatrix}$$

$$D_{i,i} = \sum_j A_{i,j}$$

- *Combinatorial Graph Laplacian L*: $L = D\text{-}A$
  - L is *symmetric* (graph undirected).
  - L is a *high-pass* filter.
  - L is related to *2^{nd} derivative*.

$$L = \begin{bmatrix} w_{1,2} & -w_{1,2} & 0 & 0 \\ -w_{1,2} & w_{1,2}+1 & -1 & 0 \\ 0 & -1 & 2 & -1 \\ 0 & 0 & -1 & 1 \end{bmatrix}$$

$$L_{3,:}x = -x_2 + 2x_3 - x_4$$

$$f''(x) = \lim_{h \to 0} \frac{f(x+h) - 2f(x) + f(x-h)}{h^2}$$

*https://en.wikipedia.org/wiki/Second_derivative

Graph Spectrum from GFT

- **Graph Fourier Transform** (GFT) is eigen-matrix of graph Laplacian L.

eigenvalues along diagonal

$$\mathbf{L} = \mathbf{V}\,\Sigma\,\mathbf{V}^T$$

GFT

eigenvectors in columns

$$\tilde{\mathbf{x}} = \mathbf{V}^T\mathbf{x}$$

GFT coefficients

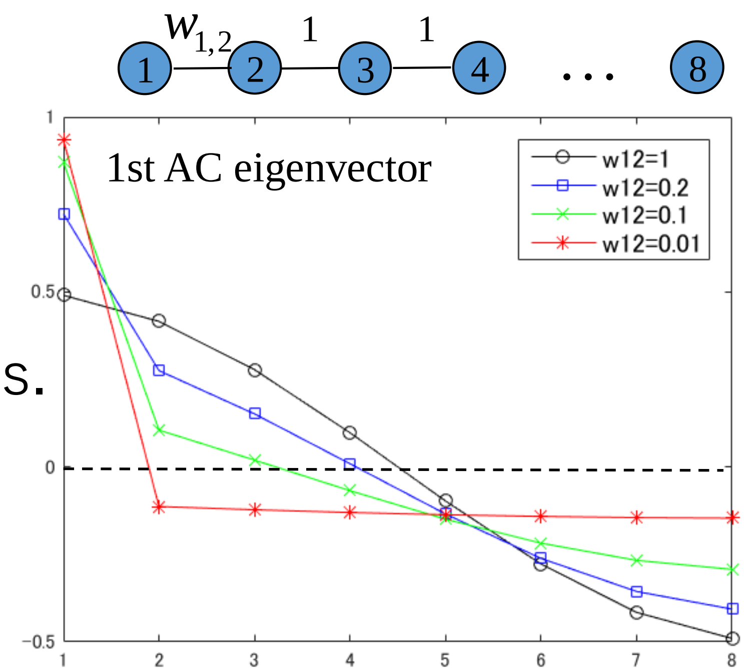

1. Edge weights affect shapes of eigenvectors.
2. Eigenvalues (≥ 0) as *graph frequencies*.
   - Constant eigenvector is DC.
   - \# *zero-crossings* increases as λ increases.

- GFT defaults to *DCT* for un-weighted connected line.
- GFT defaults to *DFT* for un-weighted connected circle.

Variants of Graph Laplacians

- **Graph Fourier Transform** (GFT) is eigen-matrix of graph Laplacian L.

eigenvalues along diagonal

$$\mathrm{L} = \mathrm{V}\,\Sigma\,\mathrm{V}^T$$

GFT

eigenvectors in columns

- Other definitions of graph Laplacians:
  - **Normalized** graph Laplacian:

$$L_n = D^{-1/2} L D^{-1/2} = I - D^{-1/2} A D^{-1/2}$$

  - **Random walk** graph Laplacian:

$$L_{rw} = D^{-1} L = I - D^{-1} A$$

  - **Generalized** graph Laplacian [1]:

$$L_g = L + D^*$$

Characteristics:

- Normalized.
- Symmetric.
- No DC component.

- Normalized.
- Asymmetric.
- Eigenvectors not orthog.

- Symmetric.
- **L** plus self loops.
- Defaults to DST, ADST.

[1] Wei Hu, Gene Cheung, Antonio Ortega, "**Intra-Prediction and Generalized Graph Fourier Transform for Image Coding**," *IEEE Signal Processing Letters*, vol.22, no.11, pp. 1913-1917, November 2015.

GSP and Graph-related Research

GSP: SP framework that unifies concepts from multiple fields.

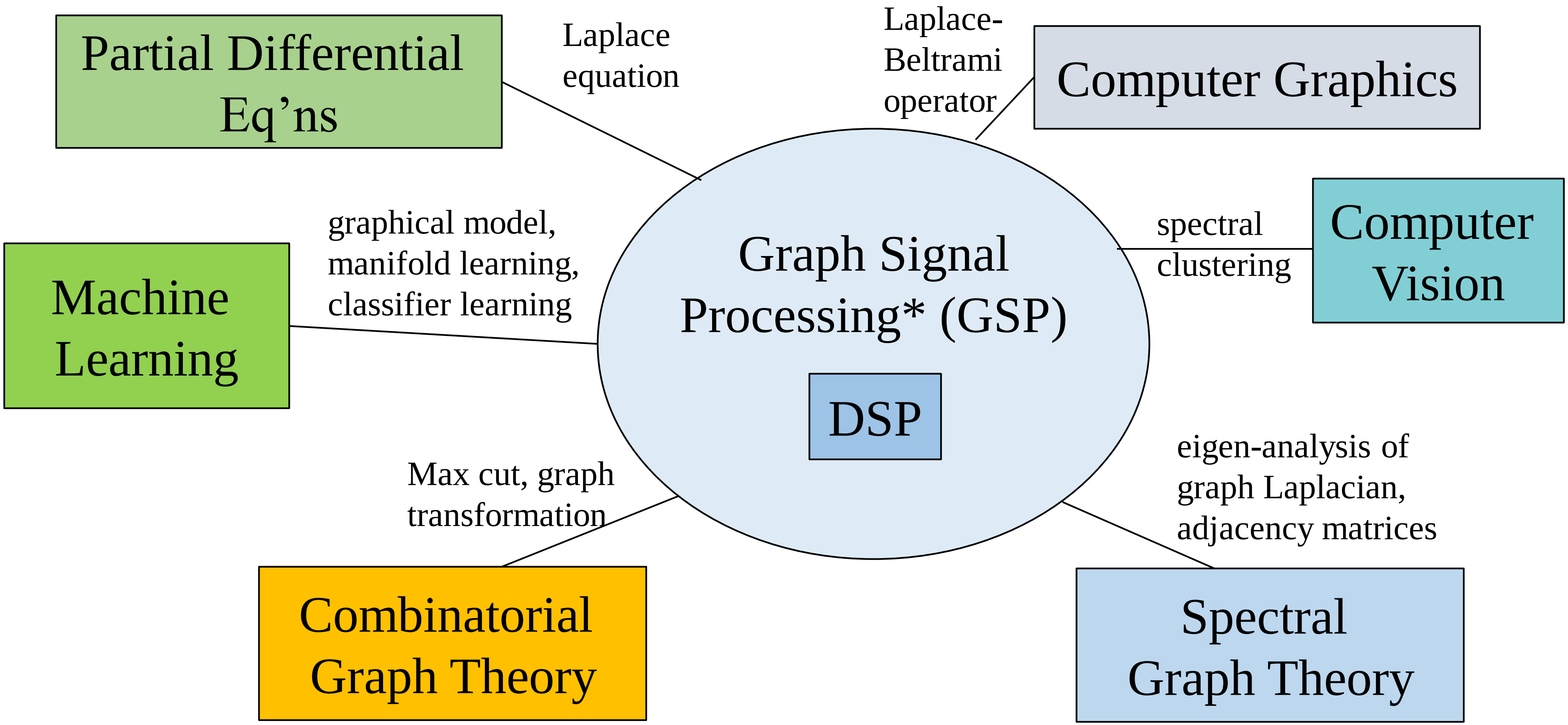

Outline

- GSP Fundamentals
- GSP for Image Compression
  - Optimality of GFT
- GSP for Inverse Imaging
  - Graph Laplacian Regularizer
  - Reweighted Graph TV
- Deep GLR
- Ongoing & Future Work

GFT for Image Compression

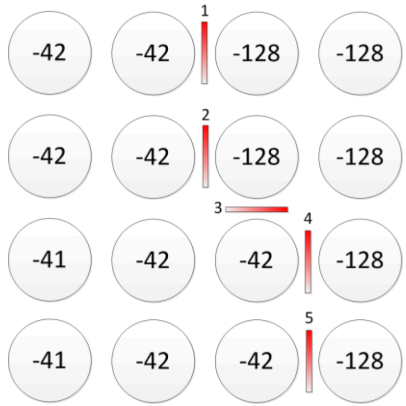

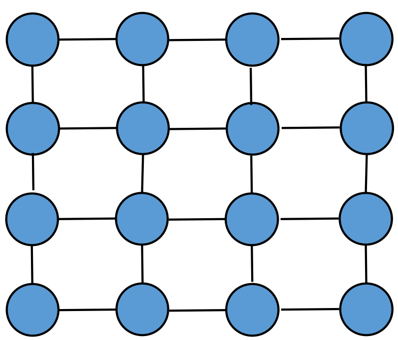

- DCT are ***fixed*** basis. Can we do better?
- **Idea**: use ***adaptive*** GFT to improve sparsity [1].

1. Assign edge weight 1 to adjacent pixel pairs.
2. Assign edge weight 0 to sharp signal discontinuity.
3. Compute GFT for transform coding, transmit coeff.

$$\tilde{\mathbf{x}} = \mathbf{V}^T \mathbf{x}$$

GFT

4. Transmit bits (*contour*) to identify chosen GFT to decoder (overhead of GFT).

[1] G. Shen et al., "**Edge-adaptive Transforms for Efficient Depth Map Coding**," *IEEE Picture Coding Symposium*, Nagoya, Japan, December 2010.

[2] W. Hu, G. Cheung, X. Li, O. Au, "**Depth Map Compression using Multi-resolution Graph-based Transform for Depth-image-based Rendering**," *IEEE International Conference on Image Processing*, Orlando, FL, September 2012.

GFT: Derivation of Optimal Edge Weights

- Assume a 1D 1st-order ***autoregressive (AR) process*** $\mathbf{x} = [x_1, \dots, x_N]^T$ where,

0-mean r.v. with large var. σ^2

$$x_k = \begin{cases} \eta & k = 1 \\ x_{k-1} + e_k & 1 < k \leq N \end{cases}$$

0-mean r.v. with var. σ_k^2

$$\mathbf{F}\mathbf{x} = \mathbf{b}, \qquad \mathbf{x} = \mathbf{F}^{-1}\mathbf{b}$$

$$\begin{aligned} x_1 &= \eta \\ x_2 - x_1 &= e_2 \\ &\vdots \\ x_N - x_{N-1} &= e_N \end{aligned} \quad \Longrightarrow \quad \mathbf{F} = \begin{bmatrix} 1 & 0 & 0 & 0 & 0 & 0 \\ -1 & 1 & 0 & 0 & 0 & 0 \\ 0 & \ddots & \ddots & 0 & 0 & 0 \\ 0 & 0 & -1 & 1 & 0 & 0 \\ 0 & 0 & 0 & \ddots & \ddots & 0 \\ 0 & 0 & 0 & 0 & -1 & 1 \end{bmatrix}, \quad \mathrm{b} = \begin{bmatrix} \eta \\ e_2 \\ \vdots \\ \\ \\ e_N \end{bmatrix}$$

GFT: Derivation of Optimal Edge Weights

- Covariance matrix

$$\mathbf{C} = E\left[(\mathrm{x}-\mu)(\mathrm{x}-\mu)^T\right] = E\left[\mathrm{x}\,\mathrm{x}^T\right] = E\left[\mathbf{F}^{-1}\mathrm{b}\,\mathrm{b}^T\left(\mathbf{F}^{-1}\right)^T\right] = \mathbf{F}^{-1}E\left[\mathrm{b}\,\mathrm{b}^T\right]\left(\mathbf{F}^{-1}\right)^T$$

$$E\left[\mathbf{bb}^T\right] = \begin{bmatrix} \sigma^2 & 0 & \cdots & 0 \\ 0 & \sigma_2^2 & & \vdots \\ \vdots & & \ddots & 0 \\ 0 & \cdots & 0 & \sigma_N^2 \end{bmatrix}$$

- Precision matrix (tri-diagonal)

large

$$\mathrm{Q} = \mathrm{C}^{-1} = \begin{bmatrix} \frac{1}{\sigma^2}+\frac{1}{\sigma_2^2} & -\frac{1}{\sigma_2^2} & 0 & \cdots & 0 \\ -\frac{1}{\sigma_2^2} & \frac{1}{\sigma_2^2}+\frac{1}{\sigma_3^2} & -\frac{1}{\sigma_2^2} & & \vdots \\ 0 & \ddots & \ddots & \ddots & 0 \\ \vdots & & -\frac{1}{\sigma_{N-1}^2} & \frac{1}{\sigma_{N-1}^2}+\frac{1}{\sigma_N^2} & -\frac{1}{\sigma_N^2} \\ 0 & \cdots & 0 & -\frac{1}{\sigma_N^2} & \frac{1}{\sigma_N^2} \end{bmatrix} \approx \mathbf{L}$$

Graph Laplacian matrix!

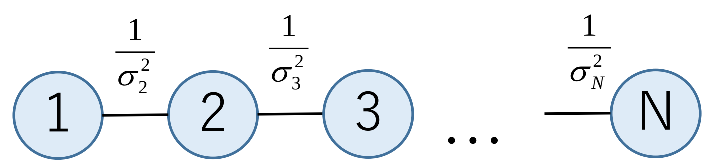

GFT for PWS Image Coding

- Graph Laplacian ≈ Precision Matrix → GFT approx. *Karhunen-Loeve Transform* (KLT).

- Encode blocks with **signal-decorrelation** GFT.

Rate of transform coefficient vector α

Rate of transform description T

$$\min_{\mathbf{W}} \quad R_\alpha(\mathbf{x}, \mathbf{W}) + R_T(\mathbf{W})$$

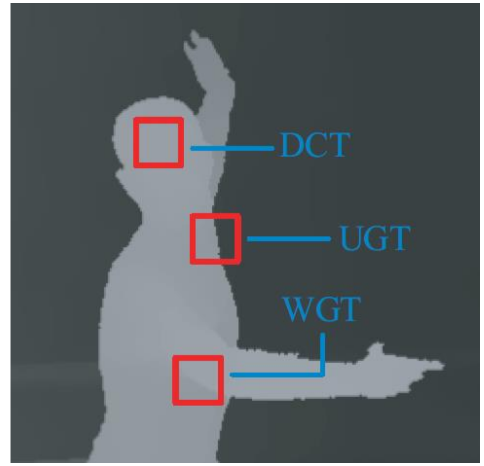

- To limit the description cost R_T, restrict weights to a small discrete set $\mathcal{C} = \{1, 0, c\}$

- "1": *strong correlation* in smooth regions
- "0": *zero correlation* in sharp boundaries
- "c": *weak correlation* in slowly-varying parts

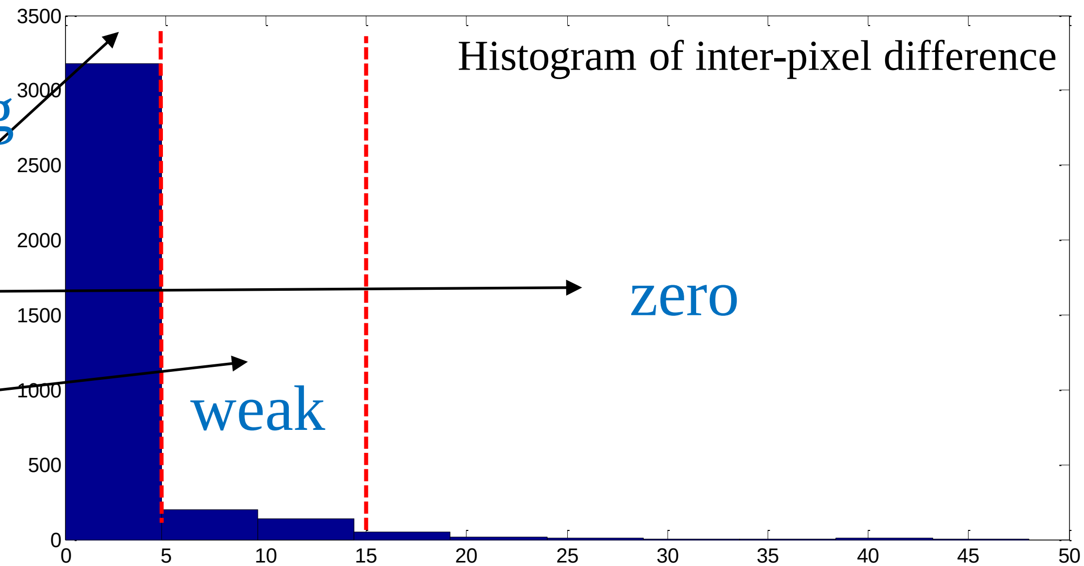

Transform Comparison

	Transform Representation	**Transform Description**
Karhunen-Loeve Transform (KLT)	"Sparsest" signal representation given available statistical model	Can be expensive (if poorly structured)
Discrete Cosine Transform (DCT)	*non-sparse signal representation* across sharp boundaries	little (fixed transform)
Graph Fourier Transform (GFT)	minimizes the total rate of signal's transform representation & transform description	

[1] Wei Hu, Gene Cheung, Antonio Ortega, Oscar Au, "**Multiresolution Graph Fourier Transform for Compression of Piecewise Smooth Images**," *IEEE Transactions on Image Processing*, vol.24, no.1, pp.419-433, January 2015.

Experimentation

- Setup
  - Test images: depth maps of *Teddy* and *Cones*, and graphics images of *Dude* and *Tsukuba*.
  - Compare against: HR-DCT, HR-SGFT, SAW, MR-SGFT in H.264.
- Results

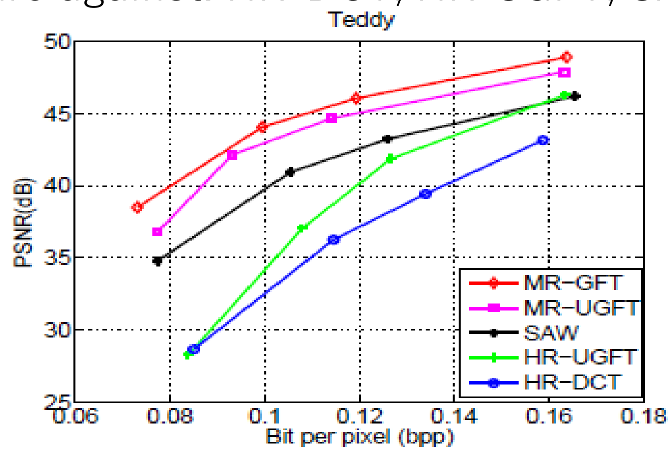

(a)

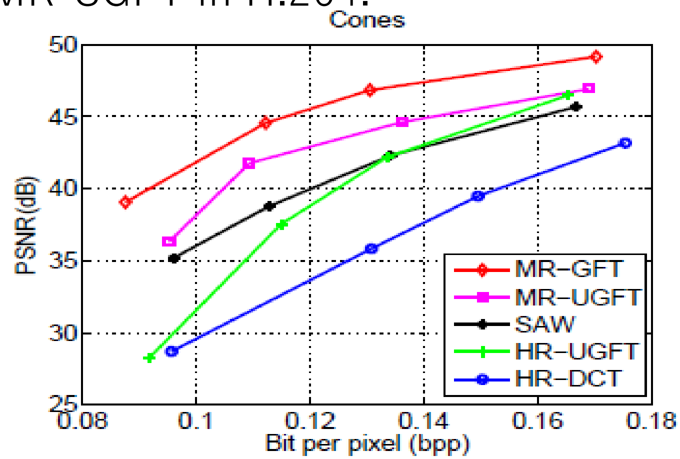

(b)

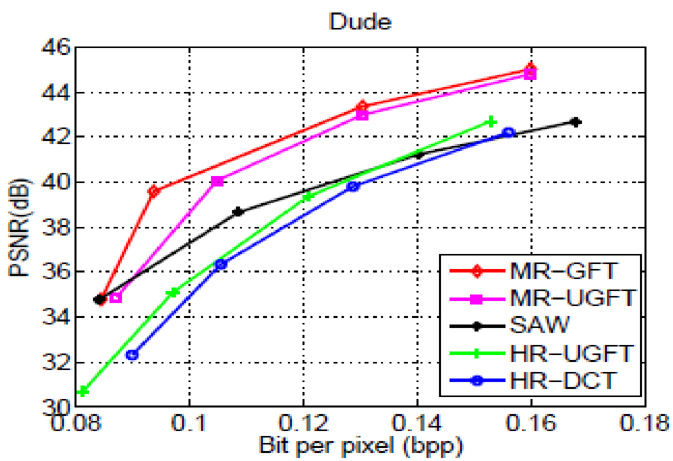

(c)

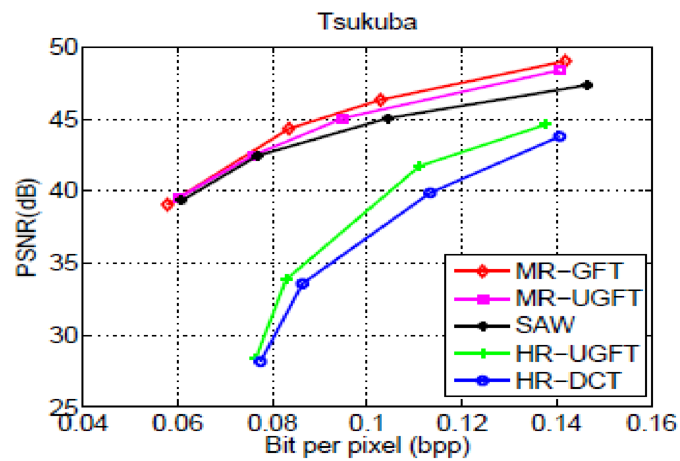

(d)

HR-DCT:	6.8dB
HR-SGFT:	5.9dB
SAW:	2.5dB
MR-SGFT:	1.2dB

Subjective Results

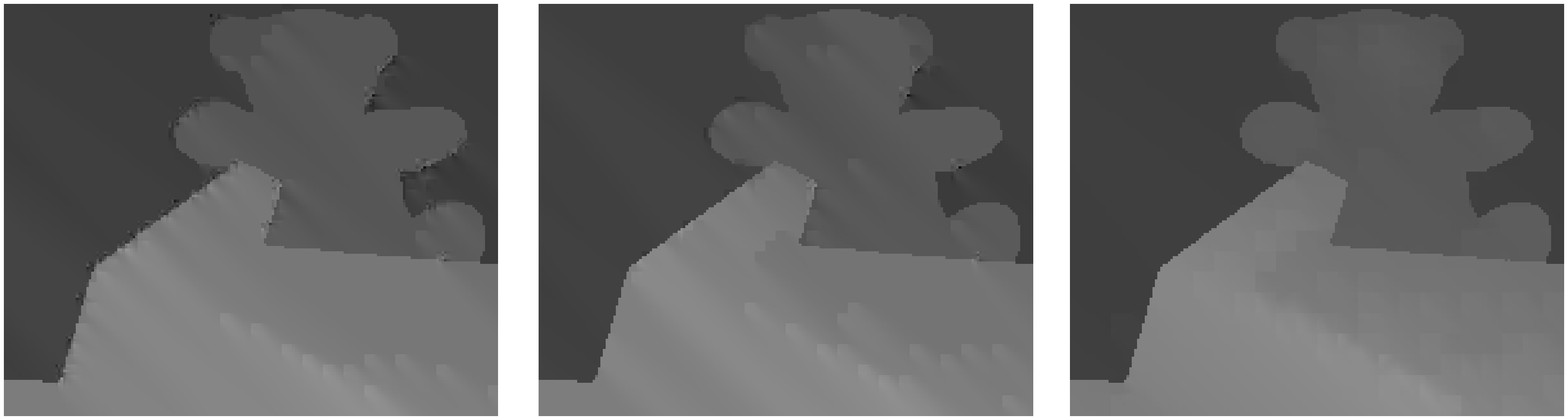

HR-DCT HR-SGFT MR-GFT

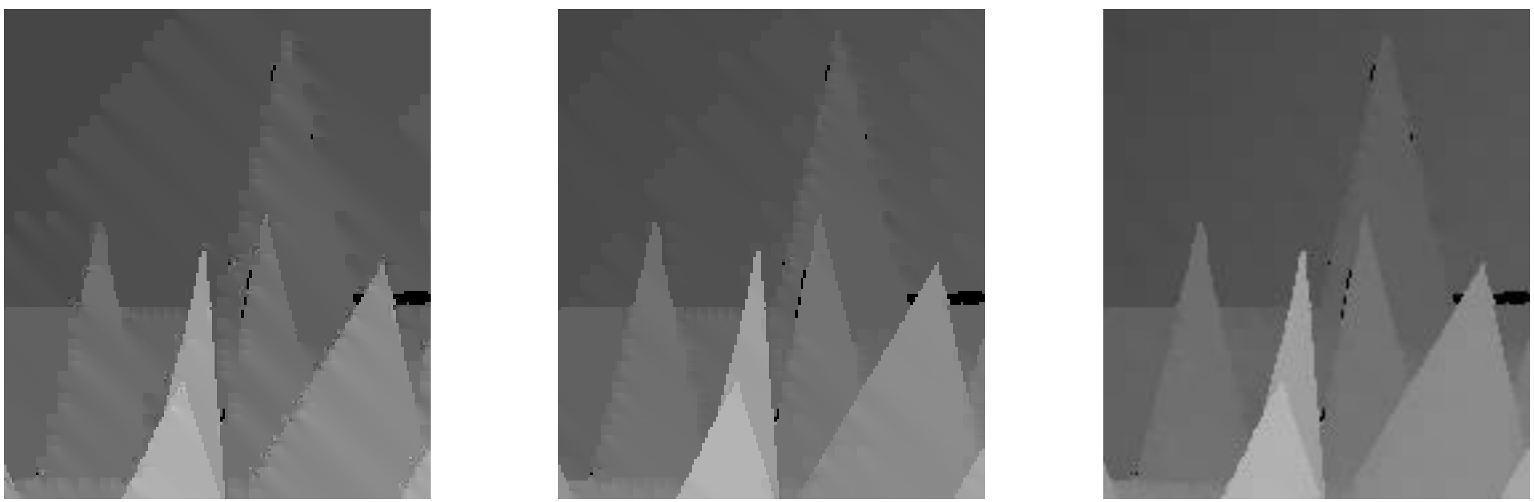

Summary of GFT for Image Coding

- Optimality of GFT for AR model.
- Variants of GFT for prediction residuals, anti-correlated pixels.
- Fast implementation (w/o eigen-decomposition) via **Graph Lifting Transform** (GLT) [1] or **Fast Graph Fourier Transform** (FGFT) [2].

[1] Y.-H. Chao et al., "Edge-Adaptive Depth Map Coding with Lifting Transform on Graphs," 31st Picture Coding Symposium, Cairns, Australia, May, 2015.

[2] L. Le Magoarou et al., "Approximate Fast Graph Fourier Transforms via Multilayer Sparse Approximations," *IEEE TSIPN*, May, 2018.

Graph-Signal Sampling / Encoding for 3D Point Cloud

MIT *dataset**

- **Problem**: Point clouds require encoding specific 3D coordinates.
- **Assumption**: smooth 2D manifold in 3D space.
- **Proposal**: progressive 3D geometry rep. as series of graph-signals.
  1. adaptively identifies new samples on the manifold surface, and
  2. encodes them efficiently as graph-signals.

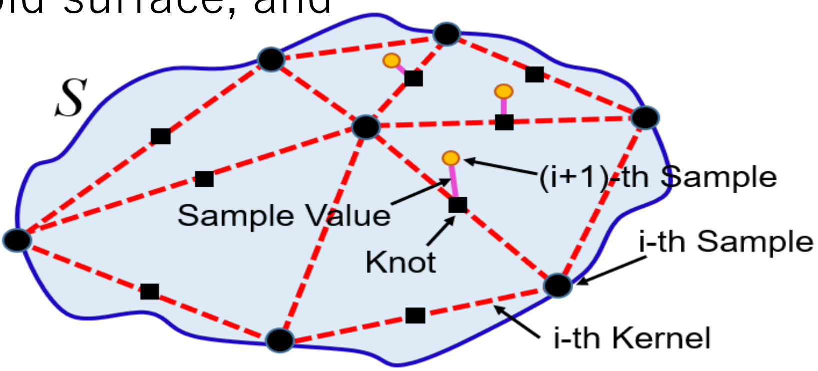

- **Example**:

1. Interpolate i^{th} iteration samples (black circles) to a **continuous kernel** (mesh), an approximation of the target surface ***S***.
2. New sample locations, **knots** (squares), are located on the kernel surface.
3. **Signed distances** between knots and ***S*** are recorded as sample values.
4. **Sample values** (green circles) are encoded as a **graph-signal via GFT**.

Graph-Signal Sampling / Encoding for 3D Point Cloud

- **Experimental Results**:

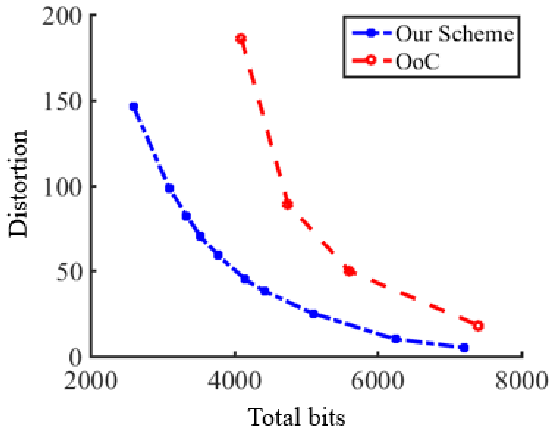

(a) Dataset1

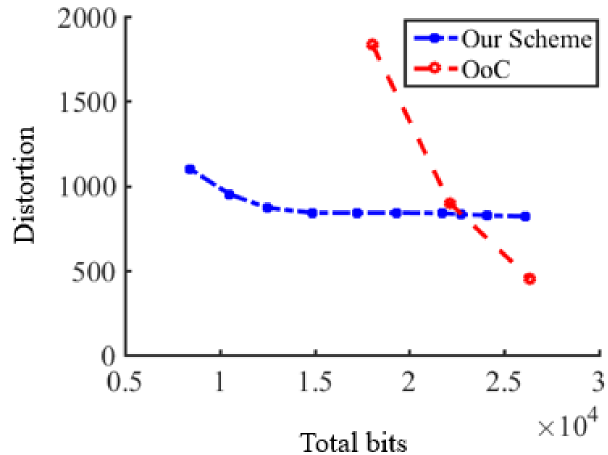

(b) Dataset2

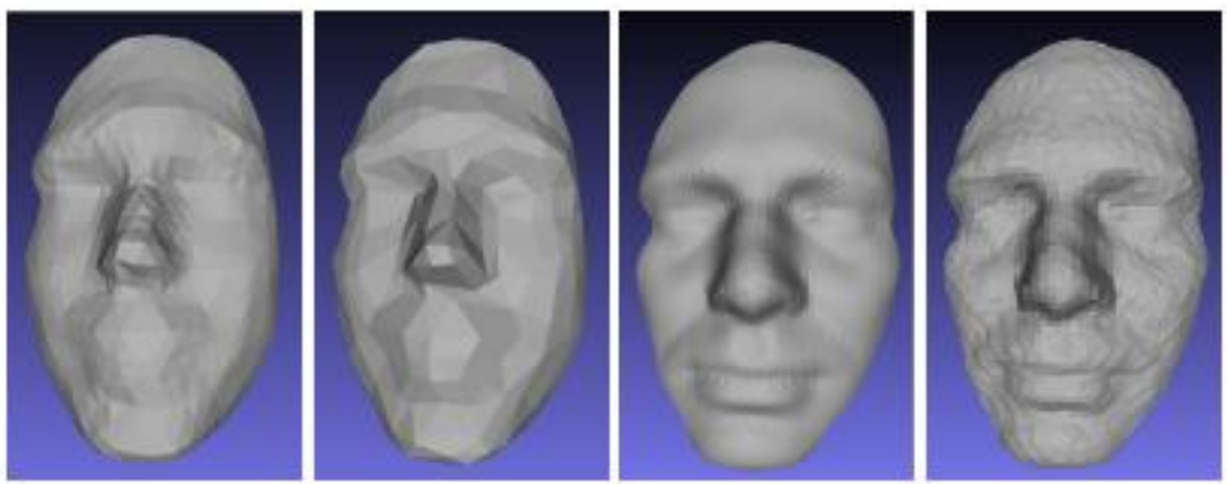

(a) (b)

[1] M. Zhao, G. Cheung, D. Florencio, X. Ji, "**Progressive Graph-Signal Sampling and Encoding for Static 3D Geometry Representation**," *IEEE International Conference on Image Processing*, Beijing, China, September, 2017.

Pre-Demosiac Light Field Image Compression Using Graph Lifting Transform

- **Problem**: Sub-aperture images in Light field data are huge.

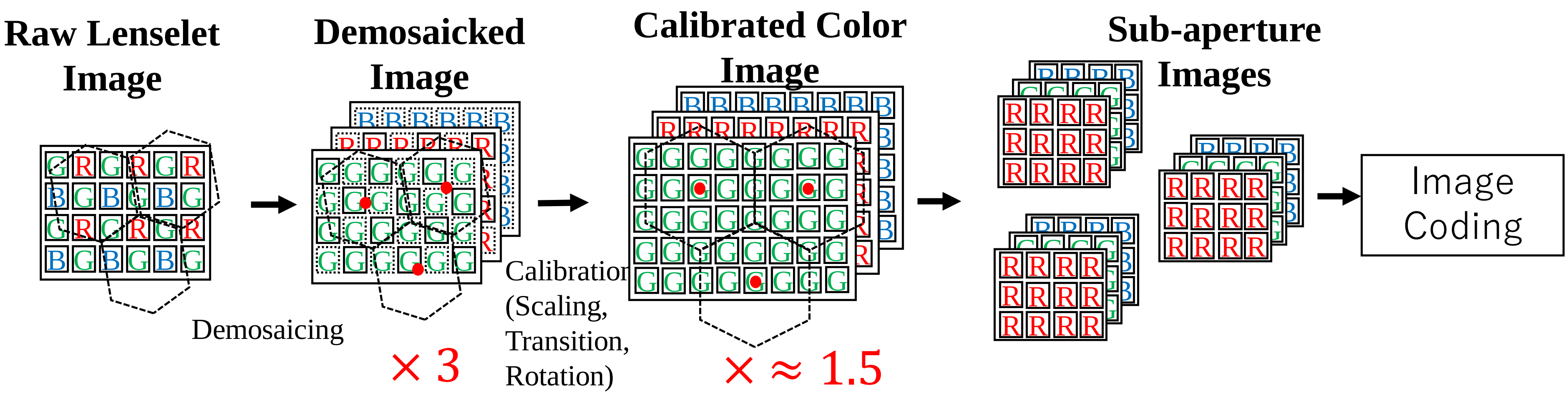

- **Proposal**: postpone demosiacking to decoder.

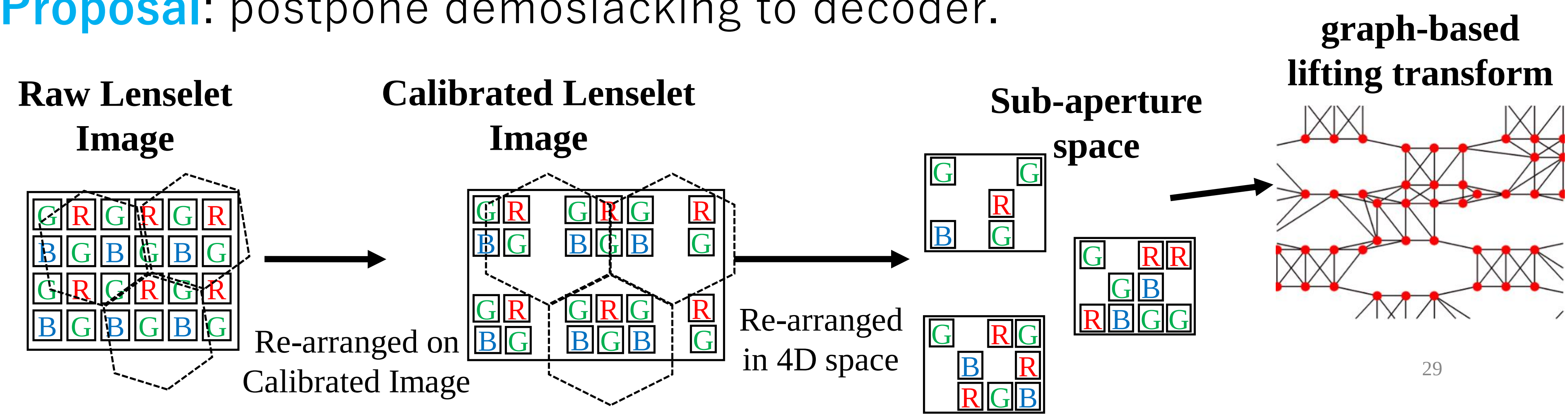

Pre-Demosiac Light Field Image Compression Using Graph Lifting Transform

- **Experimental Results**:

Dataset: EPFL light field image dataset
Baseline: All-intra HEVC coding in YUV4:2:0 and RGB 4:4:4

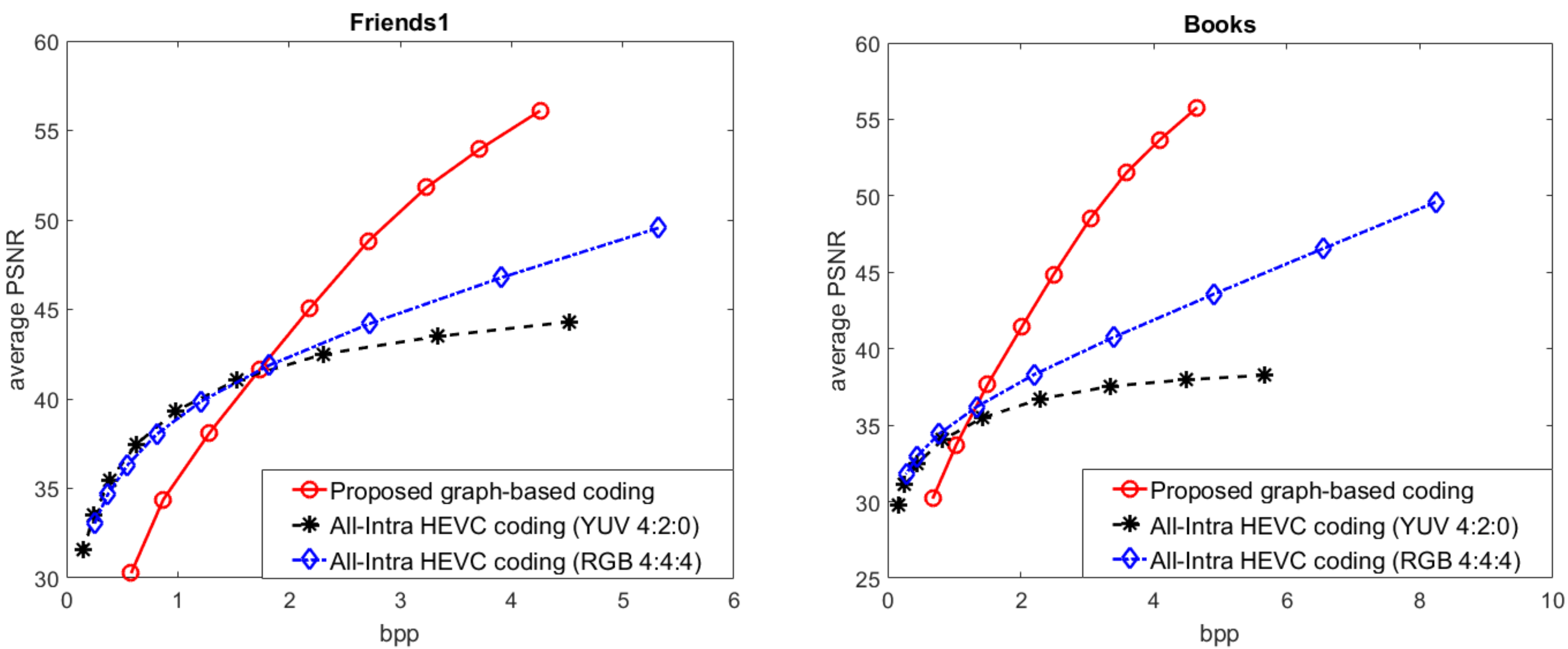

[1] Y.-H. Chao, G. Cheung, A. Ortega, "**Pre-Demosiac Light Field Image Compression Using Graph Lifting Transform**," *IEEE Int'l Conf. on Image Processing*, Beijing, China, September, 2017. (**Best student paper award**)

Outline

- GSP Fundamentals
- GSP for Image Compression
  - Optimality of GFT
- GSP for Inverse Imaging
  - Graph Laplacian Regularizer
  - Reweighted Graph TV
- Deep GLR
- Ongoing & Future Work

Graph Laplacian Regularizer

- $\mathbf{x}^T \mathbf{L} \mathbf{x}$ (graph Laplacian regularizer) [1]) is one smoothness measure.

$$\mathbf{x}^T \mathbf{L}\mathbf{x} = \frac{1}{2}\sum_{i,j} w_{i,j}\left(x_i - x_j\right)^2 = \sum_k \lambda_k \tilde{x}_k^2$$

signal smooth in nodal domain

signal contains mostly low graph freq.

- **Signal Denoising**:

observation

desired signal

$$\mathbf{y} = \mathbf{x} + \mathbf{v}$$

noise

- **MAP Formulation**:

fidelity term

$$\min_{x} \|\mathbf{y} - \mathbf{x}\|_2^2 + \mu\, \mathbf{x}^T \mathbf{L}\mathbf{x}$$

smoothness prior

update edge weights

$$\left(\mathbf{I} + \mu \mathbf{L}\right)\mathbf{x}^* = \mathbf{y}$$

linear system of eqn’s w/ sparse, symmetric PD matrix

pixel intensity diff.

pixel location diff.

$$w_{i,j} = \exp\left(\frac{-\|x_i - x_j\|_2^2}{\sigma_1^2}\right)\exp\left(\frac{-\|l_i - l_j\|_2^2}{\sigma_2^2}\right)$$

Bilateral filter weights

[1] P. Milanfar, “**A Tour of Modern Image Filtering: New Insights and Methods, Both Practical and Theoretical**,” *IEEE Signal Processing Magazine*, vol.30, no.1, pp.106-128, January 2013.

Graph Laplacian Regularizer

$$w_{i,j} = \exp\left(\frac{-\|x_i - x_j\|_2^2}{\sigma_1^2}\right)\exp\left(\frac{-\|l_i - l_j\|_2^2}{\sigma_2^2}\right)$$

- $\mathbf{x}^T \mathbf{L}(\mathbf{x})\mathbf{x}$ promotes ***piecewise smooth*** (PWS) signal behavior [1].

$$\mathbf{x}^T \mathbf{L}(\mathbf{x})\mathbf{x} = \frac{1}{2}\sum_{i,j} w_{i,j}\left(x_i - x_j\right)^2 = \frac{1}{2}\sum_{i,j} u_{i,j} \exp\left\{-\frac{\left(x_i - x_j\right)^2}{\sigma^2}\right\}\left(x_i - x_j\right)^2$$

- **Spectral Clustering** [2]:

Rayleigh quotient

$$\mathbf{v}^* = \arg\min_{\mathbf{v}} \frac{\mathbf{v}^T \mathbf{L}_\mathrm{n} \mathbf{v}}{\mathbf{v}^T \mathbf{v}} \quad s.t.\ \mathbf{v}^T \mathbf{v}_1 = 0$$

- v_1 minimizes obj → Sol’n is 2nd eigenvector of L_n.
- 2nd eigenvalue—**Fiedler number**—measures “connectedness”.
- PWS signal = 2 clusters of similar nodes → $\mathbf{x}^T \mathbf{L}\mathbf{x} \approx 0$

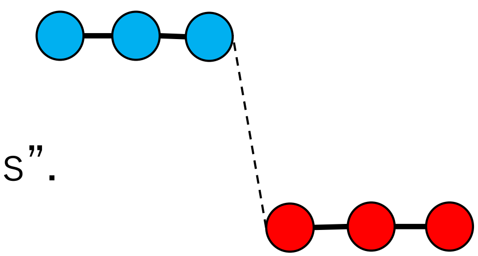

[1] X. Liu, G. Cheung, X. Wu, D. Zhao, "**Random Walk Graph Laplacian based Smoothness Prior for Soft Decoding of JPEG Images**," *IEEE Transactions on Image Processing*, vol.26, no.2, pp.509-524, February 2017.

[2] J. Shi and J. Malik, “**Normalized cuts and image segmentation**,” *IEEE Trans. Pattern Anal. Mach. Intell.*, vol. 22, no. 8, pp. 888–905, Aug. 2000.

Analysis of Graph Laplacian Regularizer

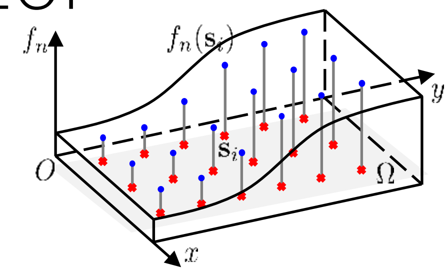

- [1] shows $S_{\mathrm{G}}(\mathbf{u}) = \mathbf{u}^{\mathrm{T}}\mathbf{L}\mathbf{u}$ converges to continuous functional S_Ω and objective becomes:

$$u^\star = \arg\min_u \|u - z_0\|_\Omega^2 + \tau \cdot \int_\Omega \nabla u^{\mathrm{T}} \mathbf{D} \nabla u \, d\mathbf{s},$$

$$\mathbf{D} = \mathbf{G}^{-1}\left(\sqrt{\det \mathbf{G}}\right)^{2\gamma - 1}$$

- Solution can be implemented as anisotropic diffusion:

feature function vector

$$\mathbf{v}_i = [\mathbf{f}_1(i)\ \mathbf{f}_2(i) \ldots \mathbf{f}_N(i)]^{\mathrm{T}}$$

$$\partial_t u = \mathrm{div}\,(\mathbf{D} \nabla u)\,,$$

$$u(\mathbf{s}, t = 0) = z_0(\mathbf{s}).$$

diffusivity

distance $d_{ij}^2 = \left\|\mathbf{v}_i - \mathbf{v}_j\right\|_2^2$

edge weight

$$w_{ij} = (\rho_i \rho_j)^{-\gamma} \psi(d_{ij})$$

  - it not only smooths but may also sharpens the image,
  - promote piecewise smooth images, like **total variation** (TV).

metric space $\mathbf{G} = \sum_{n=1}^{N} \nabla f_n \cdot \nabla f_n^{\mathrm{T}}$

[1] J. Pang, G. Cheung, "**Graph Laplacian Regularization for Inverse Imaging: Analysis in the Continuous Domain**," *IEEE Transactions on Image Processing*, vol. 26, no.4, pp.1770-1785, April 2017.

Outline

- GSP for Image Compression
  - Optimality of GFT
  - Generalized GFT
  - Signed GFT
- GSP for Inverse Imaging
  - Graph Laplacian Regularizer: Image Denoising
  - Reweighted Graph TV:
- Deep GLR
- Ongoing & Future Work

Optimal Graph Laplacian Regularization for Denoising

- Adopt a patch-based recovery framework, for a noisy patch $\mathbf{p}_0$
  1. Find $K-1$ patches similar to $\mathbf{p}_0$ in terms of Euclidean distance.
  2. Compute **feature functions**, leading to edge weights and Laplacian.
  3. Solve the unconstrained quadratic optimization:

$$\boxed{\mathrm{q}^* = \arg\min_{\mathrm{q}} \|\mathrm{p}_0 - \mathrm{q}\|_2^2 + \lambda \mathrm{q}^T \mathrm{L} \mathrm{q} \quad \Rightarrow \quad \mathrm{q} = (\mathrm{I} + \lambda \mathrm{L})^{-1} \mathrm{p}_0}$$

  to obtain the denoised patch.

Spatial

$$\mathbf{f}_1^D(i) = \sqrt{\sigma^2 + \alpha} \cdot x_i$$

$$\mathbf{f}_2^D(i) = \sqrt{\sigma^2 + \alpha} \cdot y_i$$

Intensity

$$\mathbf{f}_3^D = \frac{1}{K + \sigma_e^2 / \sigma_g^2} \sum_{k=0}^{K-1} \mathbf{p}_k$$

- Aggregate denoised patches to form an updated image.
- Denoise the image iteratively to gradually enhance its quality.
- Optimal Graph Laplacian Regularization for Denoising (OGLRD).

[1] J. Pang, G. Cheung, "**Graph Laplacian Regularization for Inverse Imaging: Analysis in the Continuous Domain**," *IEEE Transactions on Image Processing*, vol. 26, no.4, pp.1770-1785, April 2017.

Denoising Experiments (natural images)

- Subjective comparisons ($\sigma_I = 40$)

Original

Noisy, 16.48 dB

K-SVD, 26.84 dB

BM3D, 27.99 dB

PLOW, 28.11 dB

OGLR, 28.35 dB

Denoising Experiments (depth images)

- Subjective comparisons ($\sigma_I = 30$)

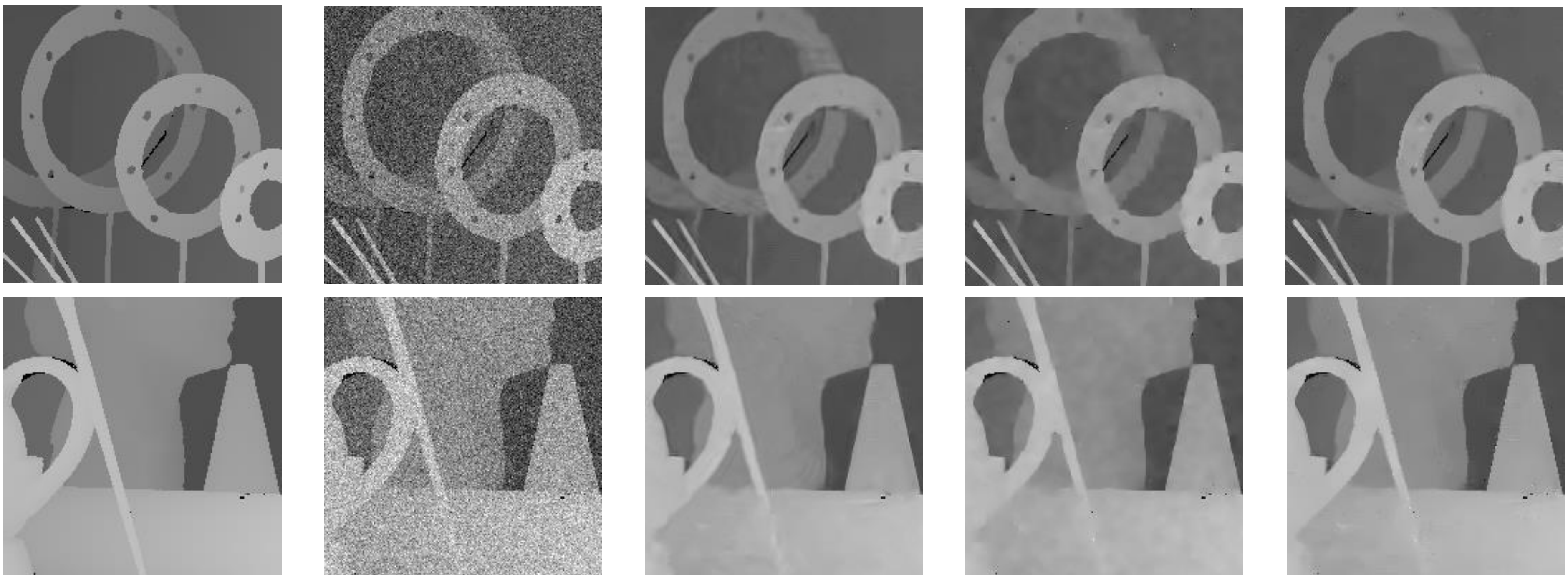

Original | Noisy, 18.66 dB | BM3D, 33.26 dB | NLGBT, 33.41dB | OGLR, 34.32 dB

[1] W. Hu et al., "**Depth Map Denoising using Graph-based Transform and Group Sparsity**," *IEEE International Workshop on Multimedia Signal Processing*, Pula (Sardinia), Italy, October, 2013.

Outline

- GSP Fundamentals
- GSP for Image Compression
  - Optimality of GFT
- GSP for Inverse Imaging
  - Graph Laplacian Regularizer
  - Reweighted Graph TV
- Deep GLR
- Ongoing & Future Work

Reweighted Graph Total Variation

- TV on graphs.

Gradient of nodes on the graph:

$$(\nabla_i \mathbf{x})_j \triangleq x_j - x_i,$$

pixel intensity difference

$$w_{i,j} = \exp\left(\frac{-\left\| x_i - x_j \right\|_2^2}{\sigma_1^2} \right)$$

Conventional Graph TV:

$$\|\mathbf{x}\|_{GTV} = \sum_{i \in \mathcal{V}} \| \operatorname{diag}(\mathbf{W}_{i,\cdot}) \nabla_i \mathbf{x} \|_1$$

$$= \sum_{i=1}^{N} \sum_{j=1}^{N} w_{i,j} |x_j - x_i|$$

Reweighted Graph TV:

$$\|\mathbf{x}\|_{RGTV} = \sum_{i \in \mathcal{V}} \| \operatorname{diag}(\mathbf{W}_{i,\cdot}(\mathbf{x})) \nabla_i \mathbf{x} \|_1$$

$$= \sum_{i=1}^{N} \sum_{j=1}^{N} w_{i,j}(x_i, x_j) |x_j - x_i|,$$

[1] M. Hidane, O. Lezoray, and A. Elmoataz, "Nonlinear multilayered representation of graph-signals," in *Journal of Mathematical Imaging and Vision*, February 2013, vol. 45, no.2, pp. 114–137.

[2] P. Berger, G. Hannak, and G. Matz, "Graph signal recovery via primal-dual algorithms for total variation minimization," in *IEEE Journal on Selected Topics in Signal Processing*, September 2017, vol. 11, no.6, pp. 842–855.

Reweighted Graph Total Variation

- RGTV is separable. analyze each node pair.
  - Promotes *bi-modal inter-pixel differences*.

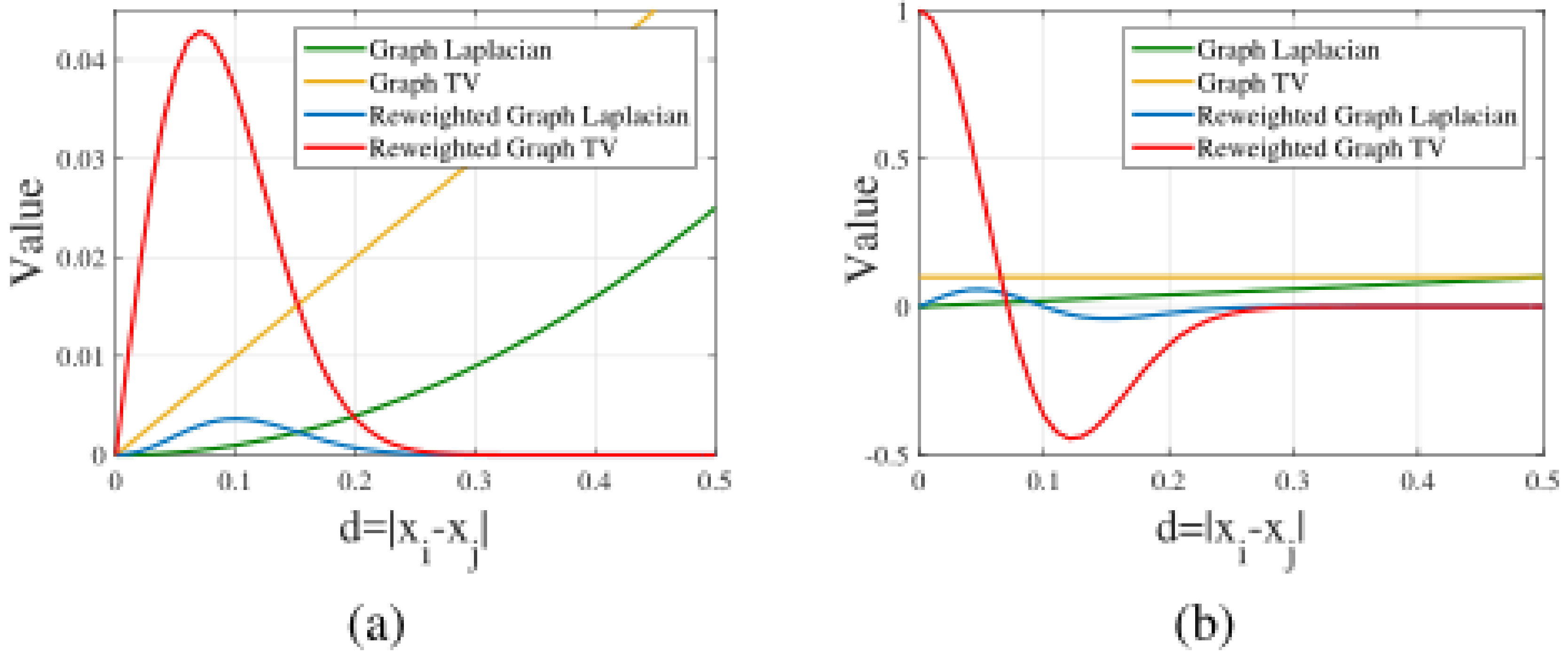

Fig. 3. Curves of regularizers and their corresponding first-derivatives for each (i, j) pair. d is normalized to $[0, 1]$. $w_{i,j} = 0.1$ for graph Laplacian and graph TV. $\sigma = 0.1$ for reweighted graph Laplacian and reweighted graph TV.

[1] Y. Bai, G. Cheung, X. Liu, W. Gao, "Blind Image Deblurring via Reweighted Graph Total Variation," *IEEE International Conference on Acoustics, Speech and Signal Processing*, Calgary, Alberta, April, 2018.

Outline

- GSP Fundamentals
- GSP for Image Compression
  - Optimality of GFT
- GSP for Inverse Imaging
  - Graph Laplacian Regularizer
  - Reweighted Graph TV: Image Deblurring
- Deep GLR
- Ongoing & Future Work

Background for Image Deblurring

- Image blur is a common image degradation.
- Typically, blur process is modeled:

$$y = k \otimes x$$

where y is the blurry image, k is the blur kernel, x is the original sharp image.

- **Blind-image deblurring** focuses on estimating blur kernel k.
- Given k, problem becomes ***de-convolution***.

Observation

- ***Skeleton image***:
  - PWS image keeping only structural edges.
  - Proxy to estimate blur kernel *k*.

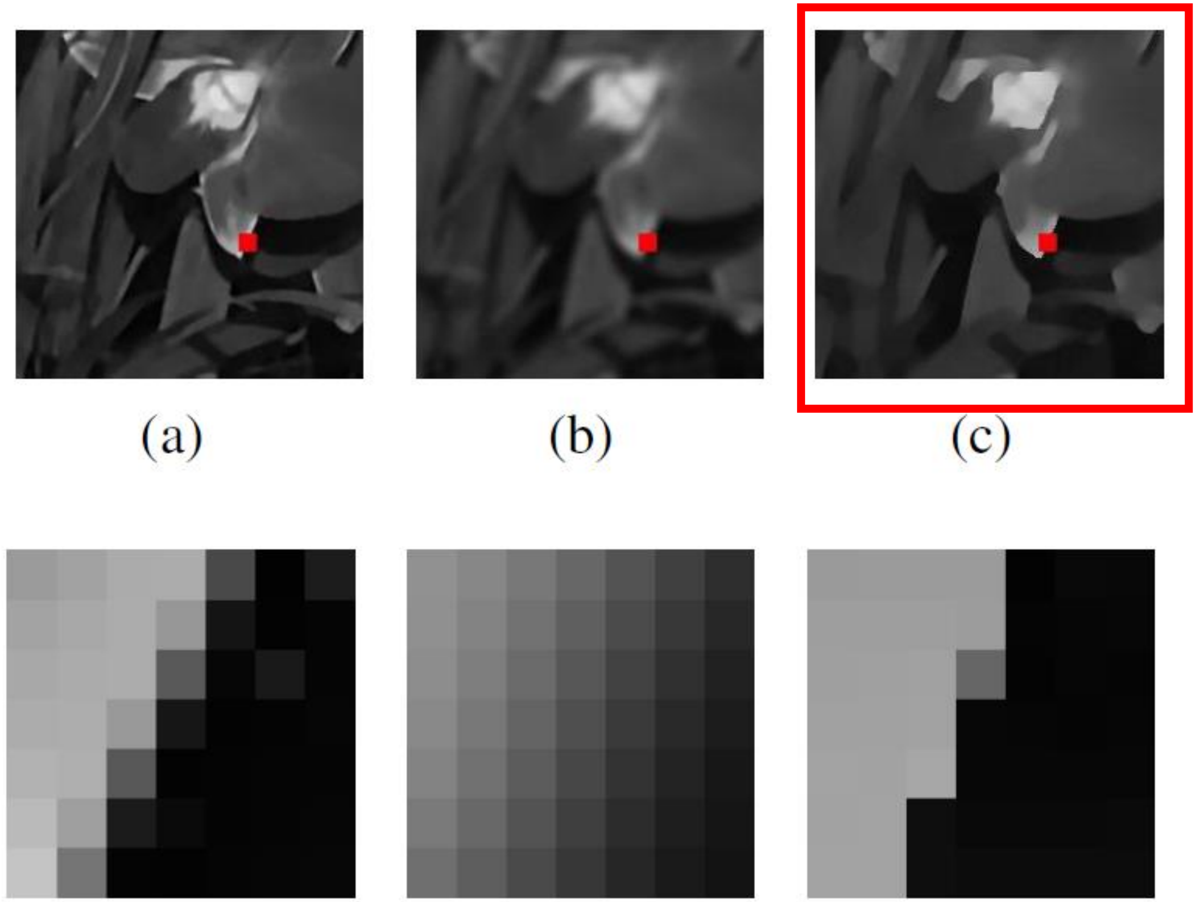

(a) (b) (c)

(d) (e) (f)

Observation

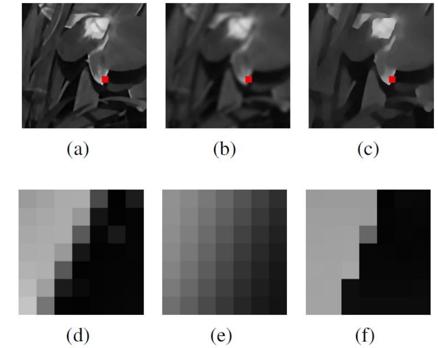

- Examine statistical properties of local patches:
  - Edge weight distribution of a fully connected graph.

$$[\mathbf{W}]_{i,j} = w_{i,j} = \exp\left(-\frac{\|x_i - x_j\|^2}{\sigma^2}\right),$$

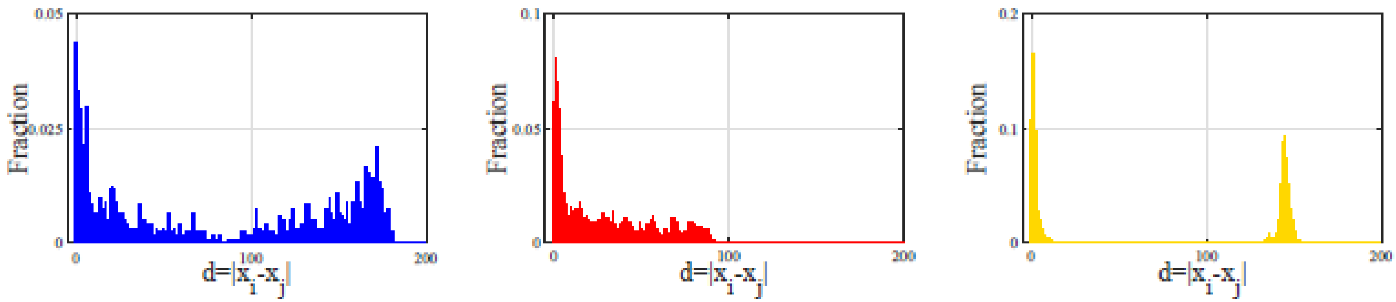

(a) (b) (c)

Fig. 2: Graph weight distribution properties around edges. (a) a true natural patch. (b) a blurry patch. (c) a skeleton patch.

- Skeleton Image enjoys both *Sharpness* and *bi-modal Weight distribution*, thus useful to estimate blur kernel.

Key Idea

- Propose a *Reweighted Graph Total Variation* (RGTV) to promote a skeleton image patch.

Conventional Graph TV:

$$\|\mathbf{x}\|_{GTV} = \sum_{i \in \mathcal{V}} \| \operatorname{diag}(\mathbf{W}_{i,\cdot}) \nabla_i \mathbf{x} \|_1 = \sum_{i=1}^{N} \sum_{j=1}^{N} w_{i,j} |x_j - x_i|$$

Reweighted Graph TV:

$$\|\mathbf{x}\|_{RGTV} = \sum_{i \in \mathcal{V}} \| \operatorname{diag}(\mathbf{W}_{i,\cdot}(\mathbf{x})) \nabla_i \mathbf{x} \|_1 = \sum_{i=1}^{N} \sum_{j=1}^{N} w_{i,j}(x_i, x_j) |x_j - x_i|,$$

Our algorithm

- The optimization function can be written as follows,

$$\hat{\mathbf{x}}, \hat{\mathbf{k}} = \underset{\mathbf{x},\mathbf{k}}{\operatorname{argmin}}\, \varphi(\mathbf{x} \otimes \mathbf{k} - \mathbf{b}) + \mu_1 \cdot \theta_x(\mathbf{x}) + \mu_2 \cdot \theta_k(\mathbf{k})$$

- Assume L_2 norm for fidelity term $\varphi(\cdot)$.
- $\theta_x(\cdot) = RGTV(\cdot)$.
- $\theta_k(\cdot) = ||\cdot||_2$, assuming zero mean Gaussian distribution of k.

- RGTV is non-differentiable and non-convex.

Solution:

- Solve x and k alternatingly.
- For x, spectral interpretation of GTV, fast spectral filter.

Spectral domain

- Deduction for spectrum of GTV

$$\left(\partial \mathbf{x}^T \mathbf{L} \mathbf{x}\right)_i = 2 \cdot (\mathbf{L}\mathbf{x})_i = c \cdot \sum_{j=1}^{N} w_{i,j} \cdot (x_i - x_j),$$
$$= c \cdot \left(\sum_{j=1}^{N} w_{i,j} x_i - \sum_{j=1}^{N} w_{i,j} x_j\right)$$

$$(\partial \|\mathbf{x}\|_{GTV})_i = c' \cdot \sum_{j=1}^{N} \gamma_{i,j} \cdot (x_i - x_j),$$
$$= c' \cdot \left(\sum_{j=1}^{N} \gamma_{i,j} x_i - \sum_{j=1}^{N} \gamma_{i,j} x_j\right)$$

$$\boxed{\gamma_{i,j} = \frac{w_{i,j}}{\max\{|x_j - x_i|, \epsilon\}}}$$

New weight function

Spectral domain

- Explanation: $\gamma_{i,j} = \dfrac{w_{i,j}}{\max\{|x_j - x_i|, \epsilon\}}$ New Adjacency matrix $\boldsymbol{\Gamma}$

$$\|\mathrm{x}\|_{GTV} = \sum_{(i,j)\in E} \gamma_{i,j} (x_i - x_j)^2$$

$$= \mathrm{x}^T \mathbf{L}_\Gamma \, \mathrm{x}$$

$$\mathbf{L}_\Gamma = \mathbf{U}_\Gamma \mathbf{\Lambda}_\Gamma \mathbf{U}_\Gamma^T$$ Graph L_1 spectrum

Our algorithm

Alternating Iterative algorithm:

$$\begin{cases} \hat{\mathbf{x}} = \mathrm{argmin}_{\mathrm{x}} \ \frac{1}{2}\left\|\mathbf{x} \otimes \widehat{\boldsymbol{k}} - \mathbf{b}\right\|_2^2 + \beta\|\mathbf{x}\|_{RGTV} \\ \hat{\mathbf{k}} = \mathrm{argmin}_{\mathrm{k}}\|\nabla\hat{\mathbf{x}} \otimes \mathbf{k} - \nabla\mathbf{b}\|_2^2 + \mu\|\mathbf{k}\|_2^2 \end{cases} \Longrightarrow \begin{array}{l} \hat{\mathbf{x}} = \mathrm{argmin}_{\mathrm{x}}\left\|\mathbf{x} \otimes \widehat{\boldsymbol{k}} - \nabla\mathbf{b}\right\|_2^2 + \beta \cdot \mathbf{x}^{\mathbf{T}}\mathbf{L}_{\Gamma}\mathbf{x} \\ \left(\widehat{\mathbf{K}}^{T}\widehat{\mathbf{K}} + 2\beta \cdot \mathbf{L}_{\Gamma}\right)\hat{\mathbf{x}} = \widehat{\mathbf{K}}^{\mathbf{T}}\mathbf{b} \end{array}$$

System of linear equations.
Efficiently solved via conjugate gradient.

Workflow

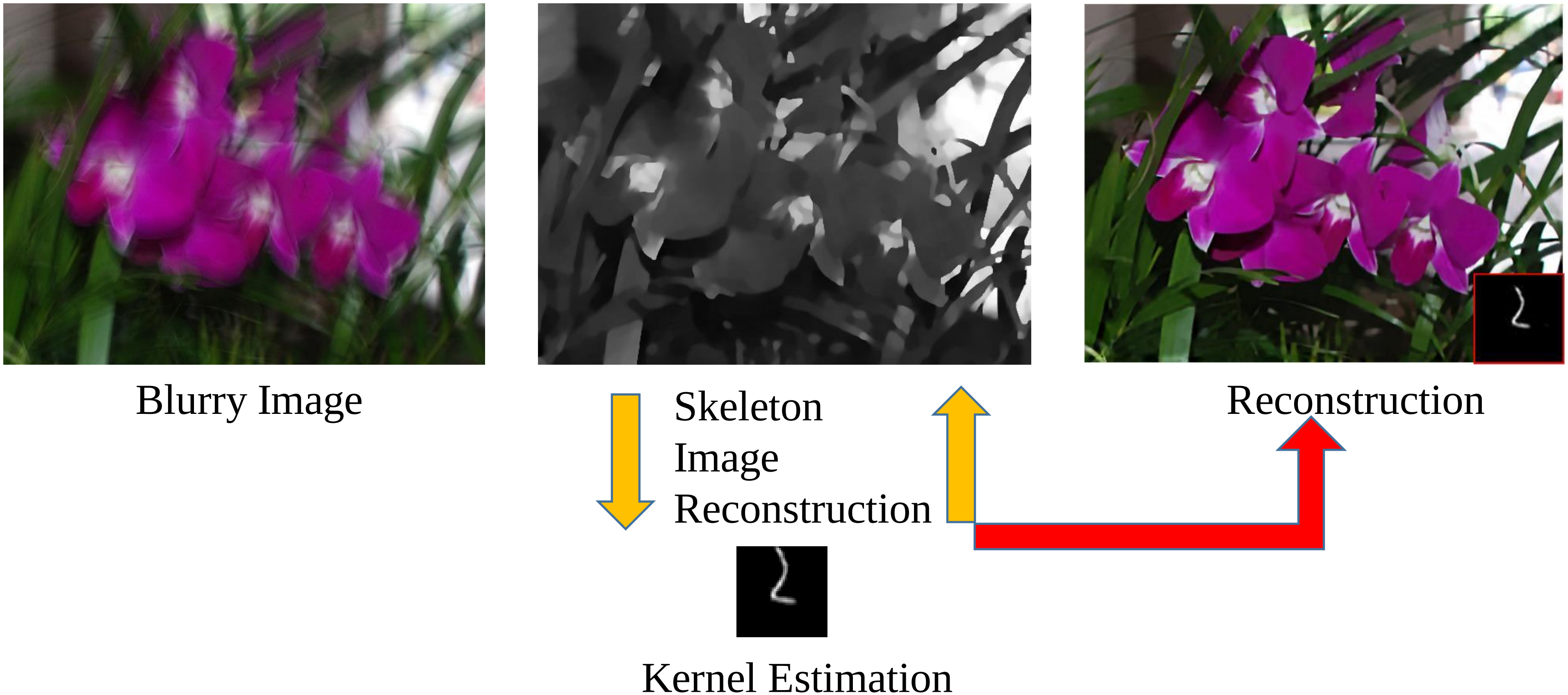
Blurry Image
Skeleton
Image
Reconstruction
Kernel Estimation
Reconstruction

Experimental Results

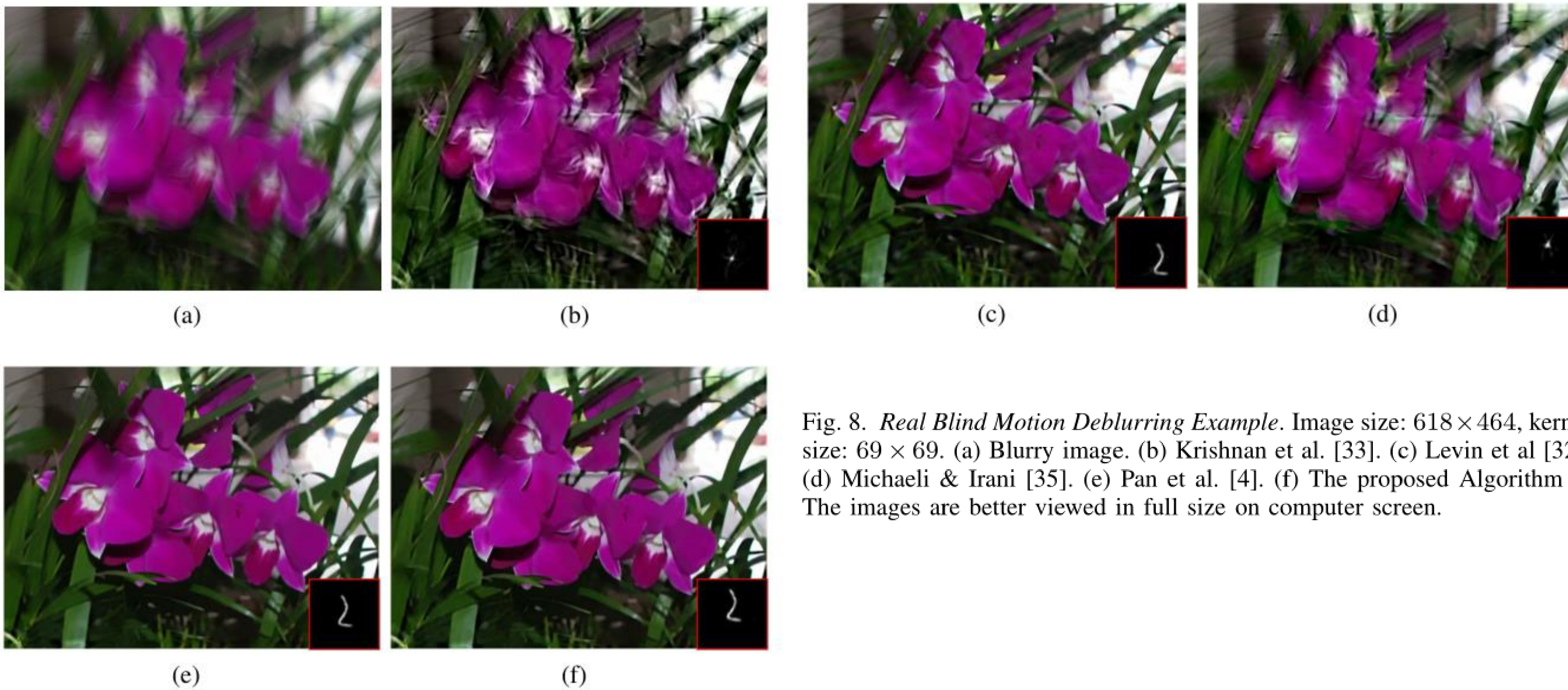

Fig. 8. *Real Blind Motion Deblurring Example*. Image size: 618×464, kernel size: 69×69. (a) Blurry image. (b) Krishnan et al. [33]. (c) Levin et al [32]. (d) Michaeli & Irani [35]. (e) Pan et al. [4]. (f) The proposed Algorithm 1. The images are better viewed in full size on computer screen.

Experimental Results

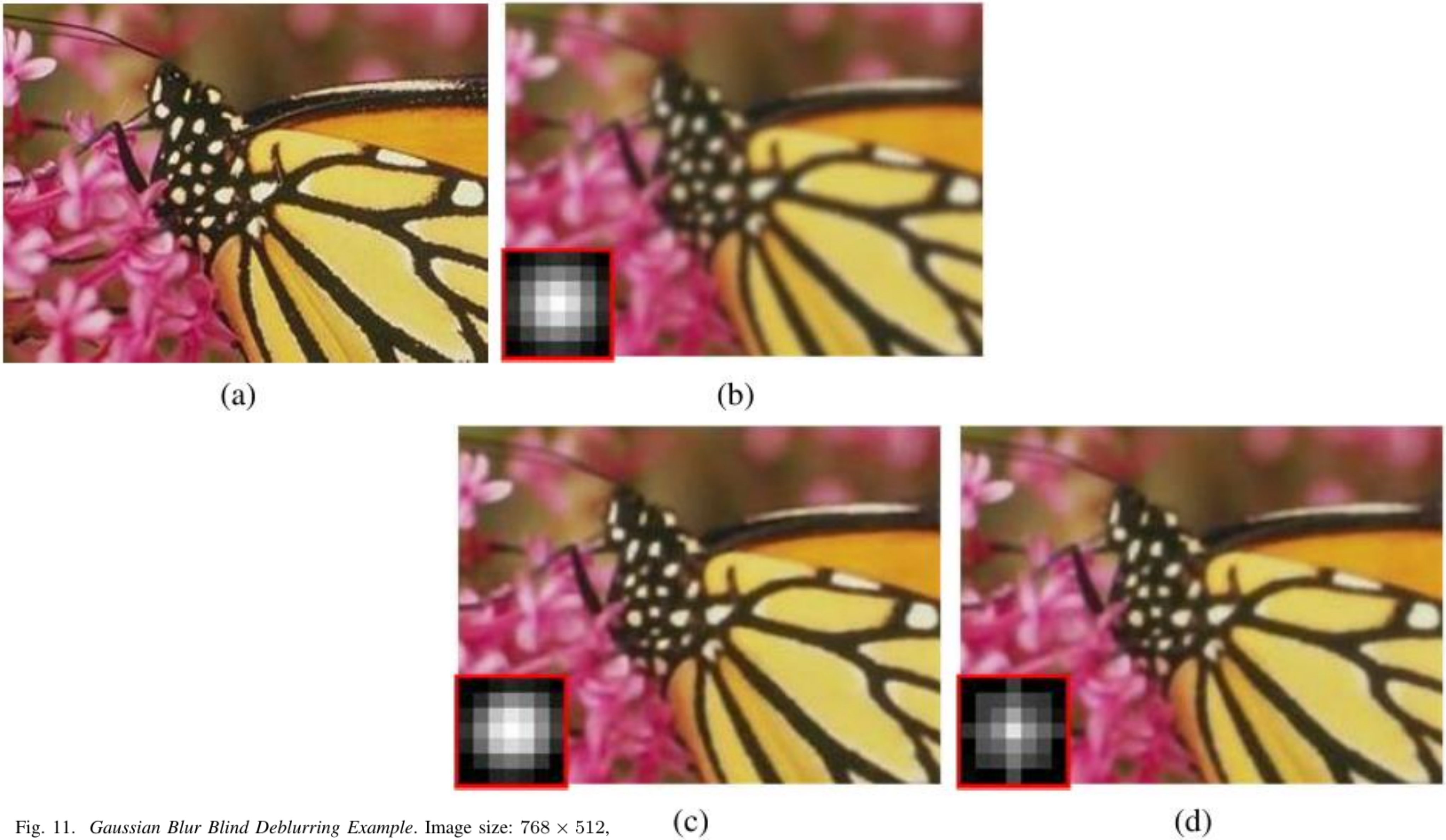

Fig. 11. *Gaussian Blur Blind Deblurring Example*. Image size: 768×512, kernel size: 7×7, $\sigma_b = 1.85$. (a) Ground-truth image. (b) Blurry image. (c) The proposed Algorithm 1. (d) The proposed Algorithm 3.

Outline

- GSP Fundamentals
- GSP for Image Compression
  - Optimality of GFT
- GSP for Inverse Imaging
  - Graph Laplacian Regularizer
  - Reweighted Graph TV: 3D Point Cloud Denoising
- Deep GLR
- Ongoing & Future Work

GTV for Point Cloud Denoising

- Acquisition of point cloud introduces noise.
- Point cloud is irregularly sampled 2D manifold in 3D space.
- Not appropriate to apply GTV directly on 3D coordinates [1].
  - only **a singular 3D point has zero GTV value**.

$$\sum_i \left| f(x_i) - f(x_{i-1}) \right|$$

functional smoothness

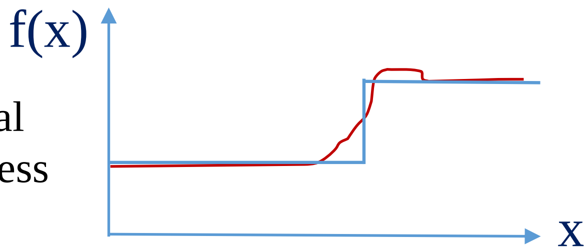

$$\sum_i \left| y_i - y_{i-1} \right| \longrightarrow \sum_i \left\| \mathrm{n}_i - \mathrm{n}_{i-1} \right\|_1$$

geometry smoothness

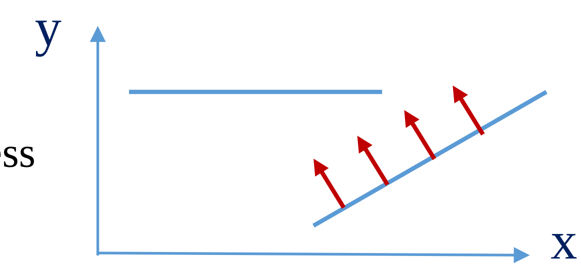

- **Proposal**: Apply GTV is to the surface normals of 3D point cloud—**a generalization of TV to 3D geometry.**

[1] Y. Schoenenberger, J. Paratte, and P. Vandergheynst, "**Graph-based denoising for time-varying point clouds**," in *IEEE 3DTV-Conference*, 2015, pp. 1–4

Algorithm Overview

- Use graph total variation (GTV) of surface normals over the K-NN graph:

$$||\mathbf{n}||_{\text{GTV}} = \sum_{i,j \in \mathcal{E}} w_{i,j} ||\mathbf{n}_i - \mathbf{n}_j||_1$$

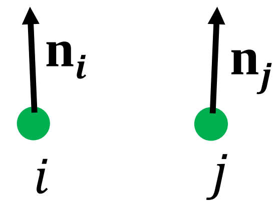

$$w_{i,j} = \exp\left(-\frac{||\mathbf{p}_i - \mathbf{p}_j||_2^2}{\sigma_p^2}\right)$$

- Denoising problem as l2-norm fidelity plus GTV of surface normals:

$$\min_{\mathrm{p,n}} \|\mathrm{q} - \mathrm{p}\|_2^2 + \gamma \sum_{i,j \in E} w_{i,j} \|\mathrm{n}_i - \mathrm{n}_j\|_1$$

- Surface normal estimation of $\mathbf{n}_i$ is a nonlinear function of $\mathbf{p}_i$ and neighbors.

Proposal:

1. Partition point cloud into **two independent classes** (say **red** and **blue**).
2. When computing surface normal for a red node, use only neighboring blue points.
3. Solve convex optimization for red (blue) nodes alternately.

[1] C. Dinesh, G. Cheung, I. V. Bajic, C. Yang, "Fast 3D Point Cloud Denoising via Bipartite Graph Approximation & Total Variation," *IEEE 20th International Workshop on Multimedia Signal Processing*, Vancouver, Canada, August 2018.

Bipartite Graph Approx. & Normal Def'n

Step 1: bipartite graph approx. of k-NN graph.

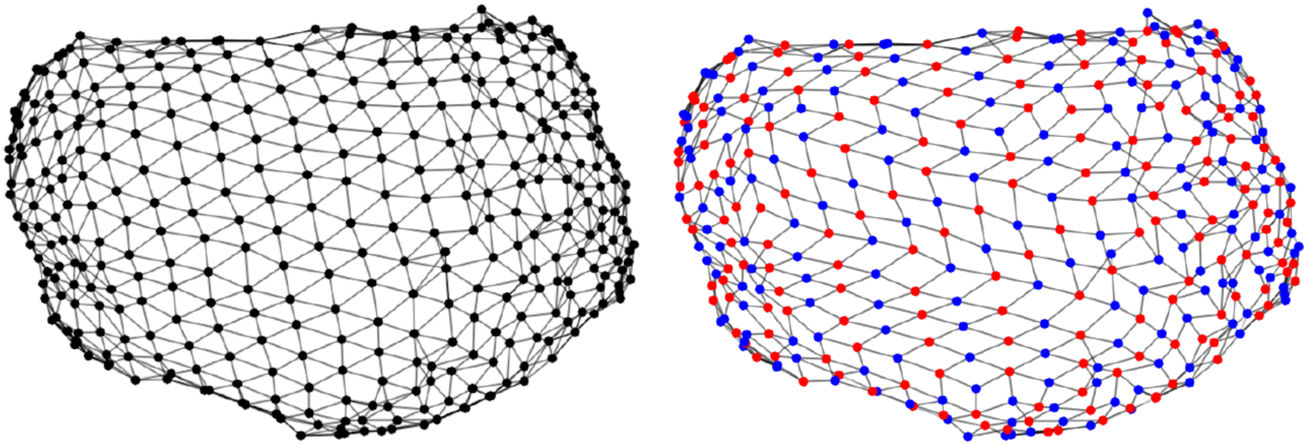

(a) original graph (b) bipartite graph

Normal vector estimation at a red node

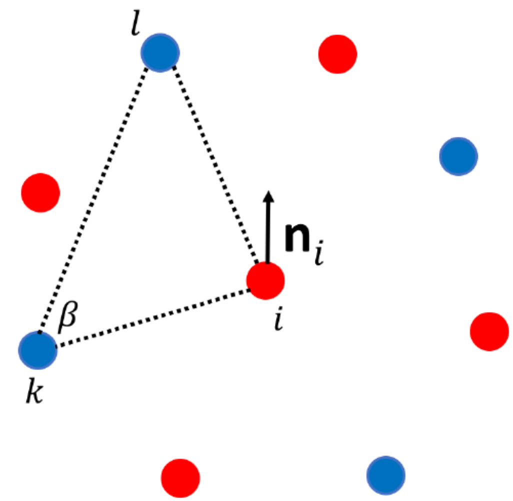

Step 2: define red nodes' normals using blue nodes.

$$\mathbf{n}_i = \frac{[\mathbf{p}_i - \mathbf{p}_k] \times [\mathbf{p}_k - \mathbf{p}_l]}{||[\mathbf{p}_i - \mathbf{p}_k] \times [\mathbf{p}_k - \mathbf{p}_l]||_2}$$

$$\mathbf{n}_i = \mathbf{A}_i \mathbf{p}_i + \mathbf{b}_i$$

$\mathbf{A}_\mathbf{i}$ is a constant matrix and $\mathbf{b}_\mathbf{i}$ is a constant vector with respect to $\mathbf{p}_\mathbf{i}$

[1] J. Zeng, G. Cheung, A. Ortega, "**Bipartite Approximation for Graph Wavelet Signal Decomposition**," *IEEE Transactions on Signal Processing*, vol.65, no.20, pp.5466-5480, October 2017.

Convex Optimization Formulation

- After computing normals for each red node, construct a new k-NN graph for red nodes only.
- For a red node graph, objective is a l2 -l1 -norm minimization w/ linear constraints:

$$\min_{\mathbf{p},\mathbf{m}} \|\mathbf{q}-\mathbf{p}\|_2^2 + \gamma \sum_{i,j\in E_r} \|\mathbf{m}_{i,j}\|_1$$

$$\mathbf{m}_{i,j} = \mathbf{n}_i - \mathbf{n}_j$$
$$\mathbf{n}_i = \mathbf{A}_i\mathbf{p}_i + \mathbf{b}_i$$
$$\mathbf{m} = \mathbf{B}\mathbf{p} + \mathbf{v}$$

Solution:

- ADMM: $\min_{\mathbf{p},\mathbf{m}} \|\mathbf{q}-\mathbf{p}\|_2^2 + \gamma \sum_{i,j\in E_r} \|\mathbf{m}_{i,j}\|_1 + \frac{\rho}{2}\|\mathbf{B}\mathbf{p}+\mathbf{v}-\mathbf{m}+\mathbf{u}\|_2^2 + \text{const}$
- p-minimization: $(2\mathbf{I}+\rho\mathbf{B}^T\mathbf{B})\mathbf{p}^{k+1} = 2\mathbf{q}+\rho\mathbf{B}^T(\mathbf{m}^k-\mathbf{u}^k-\mathbf{v}),$
- m-minimization: $\min_{\mathbf{m}} \frac{\rho}{2}\|\mathbf{B}\mathbf{p}^{k+1}+\mathbf{v}-\mathbf{m}+\mathbf{u}^k\|_2^2 + \gamma \sum_{i,j\in\mathcal{E}_1} w_{i,j}\|\mathbf{m}_{i,j}\|_1,$

Proximal gradient descent

- Alternately update red and blue graphs until convergence.

Experimental Setup

- 4 competing local methods: **APSS** [1], **RIMLS** [2], **AWLOP** [3], **MRPCA** [4]
- 7 pint cloud datasets used: Bunny, Gargoyle, DC, Daratrch, Anchor, Lordquas, Fandisk, Laurana
- Metrics: **point to point error** (C2C) and **point to plane error** (C2P)
- Gaussian noise with zero mean, standard deviation σ of 0.1 and 0.3.

[1] G. Guennebaud and M. Gross, "**Algebraic point set surfaces**," *ACM Transactions on Graphics (TOG)*, vol. 26, no. 3, p. 23, 2007.

[2] A. C. Oztireli, G. Guennebaud, and M. Gross, "**Feature preserving point set surfaces based on non-linear kernel regression**," in *Computer Graphics Forum*, vol. 28, no. 2, 2009, pp. 493–501.

[3]H. Huang, S. Wu, M. Gong, D. Cohen-Or, U. Ascher, and H. R. Zhang, "**Edge-aware point set resampling**," *ACM Transactions on Graphics*, vol. 32, no. 1, p. 9, 2013.

[4] E. Mattei and A. Castrodad, "**Point cloud denoising via moving RPCA**," in *Computer Graphics Forum*, vol. 36, no. 8, 2017, pp. 123–137.

Experimental Results – Visual Comparison

Anchor model (σ=0.3)

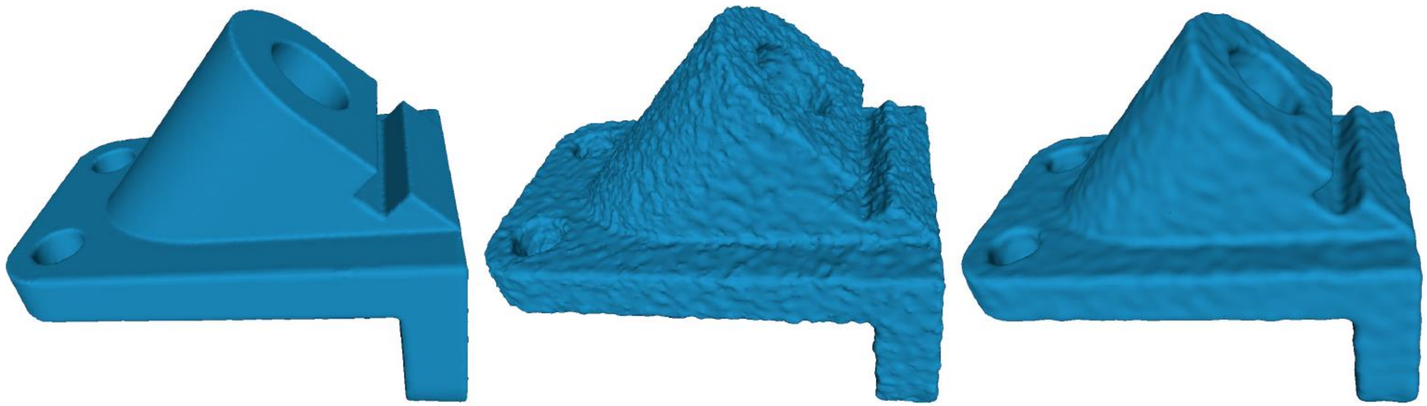

(a) ground truth (b) noisy input (c) APSS

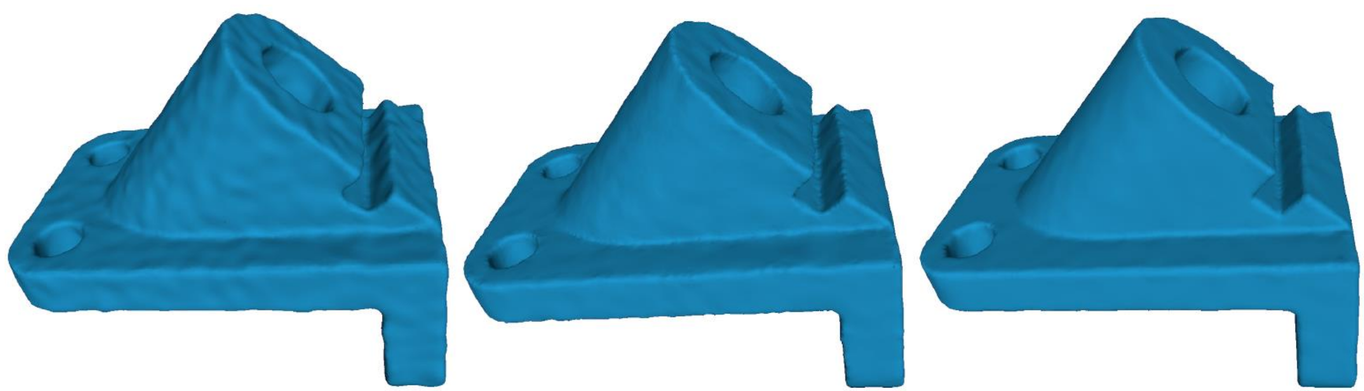

(d) RIMLS (e) MRPCA (f) proposed

Experimental Results – Visual Comparison

Daratech model (σ=0.3)

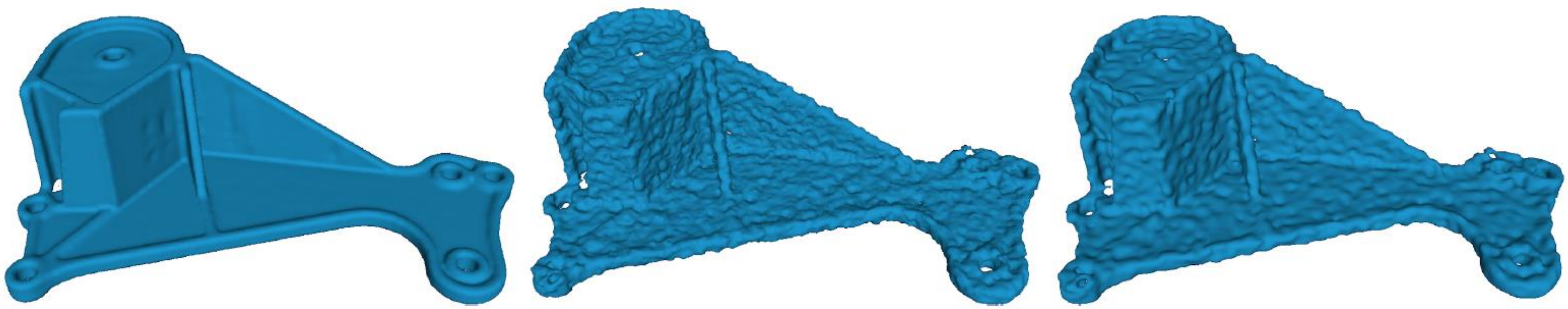

(a) ground truth (b) noisy input (c) APSS

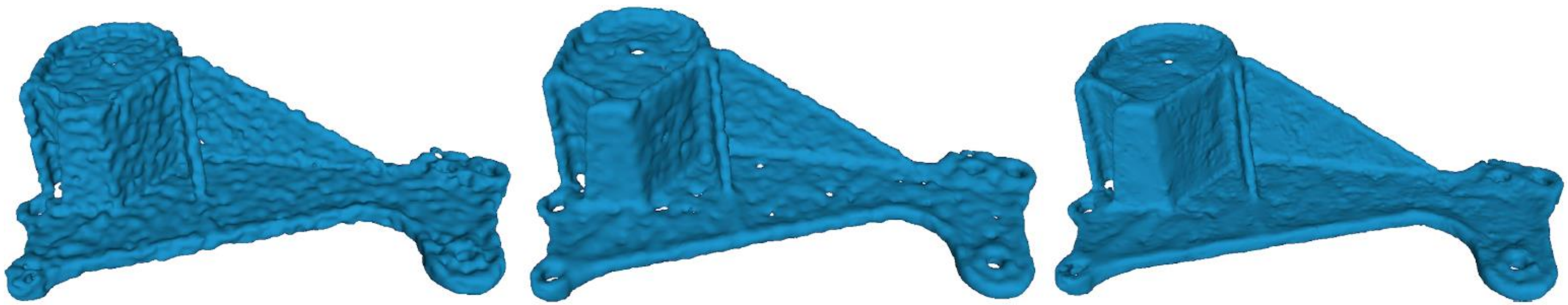

(d) RIMLS (e) MRPCA (f) proposed

Experimental Results – Numerical Comparison

TABLE I

C2C OF DIFFERENT MODELS, WITH GAUSSIAN NOISE ($\sigma = 0.1$)

Model	Noise	APSS	RIMLS	AWLOP	MRPCA	Prop.
Bunny	0.157	0.135	0.143	0.153	0.141	**0.128**
Gargoyle	0.154	0.133	0.143	0.151	0.144	**0.131**
DC	0.154	0.130	0.140	0.148	0.136	**0.128**
Daratech	0.156	0.134	0.137	0.156	0.134	**0.132**
Anchor	0.156	0.134	0.139	0.152	0.130	**0.127**
Lordquas	0.155	0.130	0.143	0.153	0.132	**0.126**
Fandisk	0.159	0.148	0.148	0.157	0.138	**0.136**
Laurana	0.150	0.136	0.139	0.147	**0.130**	**0.130**

TABLE II

C2C OF DIFFERENT MODELS, WITH GAUSSIAN NOISE ($\sigma = 0.3$)

Model	Noise	APSS	RIMLS	AWLOP	MRPCA	Prop.
Bunny	0.329	0.235	0.251	0.315	0.243	**0.231**
Gargoyle	0.304	0.220	0.232	0.288	0.218	**0.214**
DC	0.305	0.213	0.230	0.302	0.212	**0.207**
Daratech	0.313	0.264	0.268	0.293	0.262	**0.246**
Anchor	0.317	0.225	0.231	0.281	0.216	**0.210**
Lordquas	0.307	0.212	0.228	0.284	0.208	**0.203**
Fandisk	0.406	0.352	0.343	0.390	0.331	**0.319**
Laurana	0.318	0.239	0.249	0.266	0.242	**0.231**

TABLE III

C2P ($\times 10^{-3}$) OF DIFFERENT MODELS, WITH GAUSSIAN NOISE ($\sigma = 0.1$)

Model	Noise	APSS	RIMLS	AWLOP	MRPCA	Prop.
Bunny	9.91	4.62	5.14	7.95	4.66	**4.61**
Gargoyle	9.67	4.59	5.97	8.46	4.56	**4.48**
DC	9.66	4.37	4.82	7.63	3.98	**3.71**
Daratech	9.93	2.93	4.05	9.54	3.01	**2.85**
Anchor	9.87	3.32	4.10	8.43	2.18	**2.05**
Lordquas	9.72	3.33	5.81	9.10	3.79	**3.11**
Fandisk	9.88	6.70	7.05	8.93	4.86	**4.39**
Laurana	9.23	5.16	5.86	7.70	5.13	**5.01**

TABLE IV

C2P ($\times 10^{-2}$) OF DIFFERENT MODELS, WITH GAUSSIAN NOISE ($\sigma = 0.3$)

Model	Noise	APSS	RIMLS	AWLOP	MRPCA	Prop.
Bunny	6.442	1.256	1.704	5.634	1.373	**1.128**
Gargoyle	6.096	1.512	1.954	5.004	1.540	**1.499**
DC	6.130	1.349	1.738	6.097	1.391	**1.201**
Daratech	6.116	3.422	3.483	4.881	3.212	**2.215**
Anchor	6.354	1.930	2.160	3.991	1.714	**1.597**
Lordquas	6.234	1.846	2.558	4.928	1.768	**1.644**
Fandisk	7.297	3.180	2.640	6.093	1.720	**1.702**
Laurana	5.890	1.392	1.800	2.307	1.464	**1.211**

Outline

- GSP Fundamentals
- GSP for Image Compression
  - Optimality of GFT
- GSP for Inverse Imaging
  - Graph Laplacian Regularizer
  - Reweighted Graph TV: 3D Point Cloud Denoising
- Deep GLR
- Ongoing & Future Work

Unrolling Graph Laplacian Regularizer

- Recall MAP formulation of denoising problem with quadratic graph Laplacian regularizer:

$$\min_{x} \|\mathrm{y} - \mathrm{x}\|_2^2 + \mu\, \mathrm{x}^T \mathrm{L}\, \mathrm{x}$$

fidelity term

smoothness prior

- Solution is system of linear equations:

$$\left(\mathrm{I} + \mu \mathrm{L}\right) \mathrm{x}^* = \mathrm{y}$$

linear system of eqn's w/ sparse, symmetric PD matrix

Bilateral weights:

$$w_{i,j} = \exp\left(\frac{-\|x_i - x_j\|_2^2}{\sigma_1^2} \right) \exp\left(\frac{-\|l_i - l_j\|_2^2}{\sigma_2^2} \right)$$

Q: what is the "most appropriate" graph?

[1] J. Pang, G. Cheung, "**Graph Laplacian Regularization for Inverse Imaging: Analysis in the Continuous Domain**," *IEEE Transactions on Image Processing*, vol. 26, no.4, pp.1770-1785, April 2017.

Unrolling Graph Laplacian Regularizer

- **Deep Graph Laplacian Regularization:**
  1. Learn features **f**'s using CNN.
  2. Compute distance from features.
  3. Compute edge weights using Gaussian kernel.
  4. Construct graph, solve QP.

$$w_{ij} = \exp\left(-\frac{\text{dist}(i,j)}{2\epsilon^2}\right),$$

$$\text{dist}(i,j) = \sum_{n=1}^{N} \left(\mathbf{f}_n(i) - \mathbf{f}_n(j)\right)^2.$$

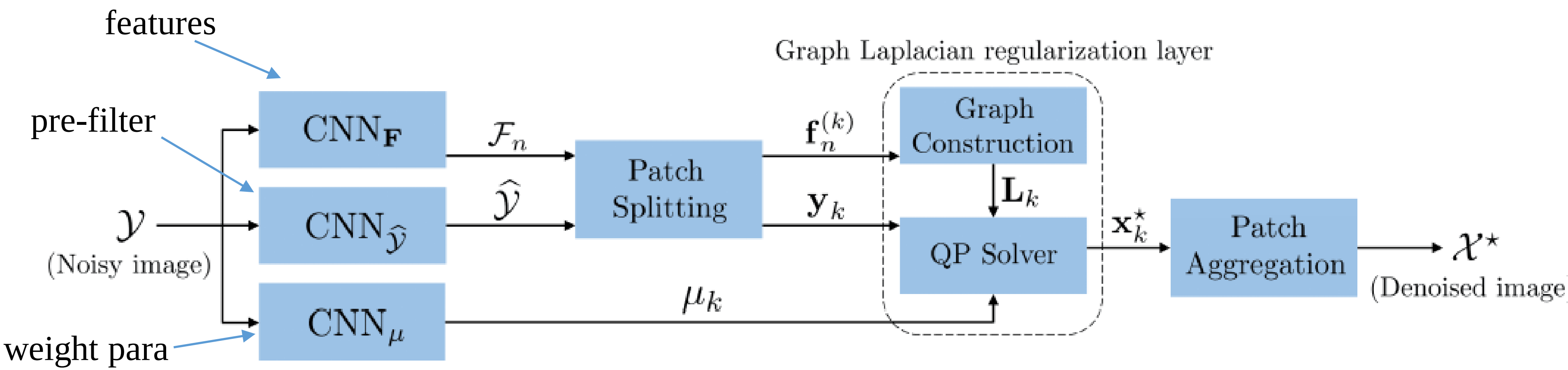

Fig. 1. Block diagram of the proposed GLRNet which employs a graph Laplacian regularization layer for image denoising.

[1] M. McCann et al., "**Convolutional Neural Networks for Inverse Problems in Imaging**," *IEEE SPM*, Nov. 2017.

[2] K. Gregor and Y. LeCun, "**Learning fast approximations of sparse coding,**" in Proc. 27th Int. Conf. Machine Learning, 2010..

Unrolling Graph Laplacian Regularizer

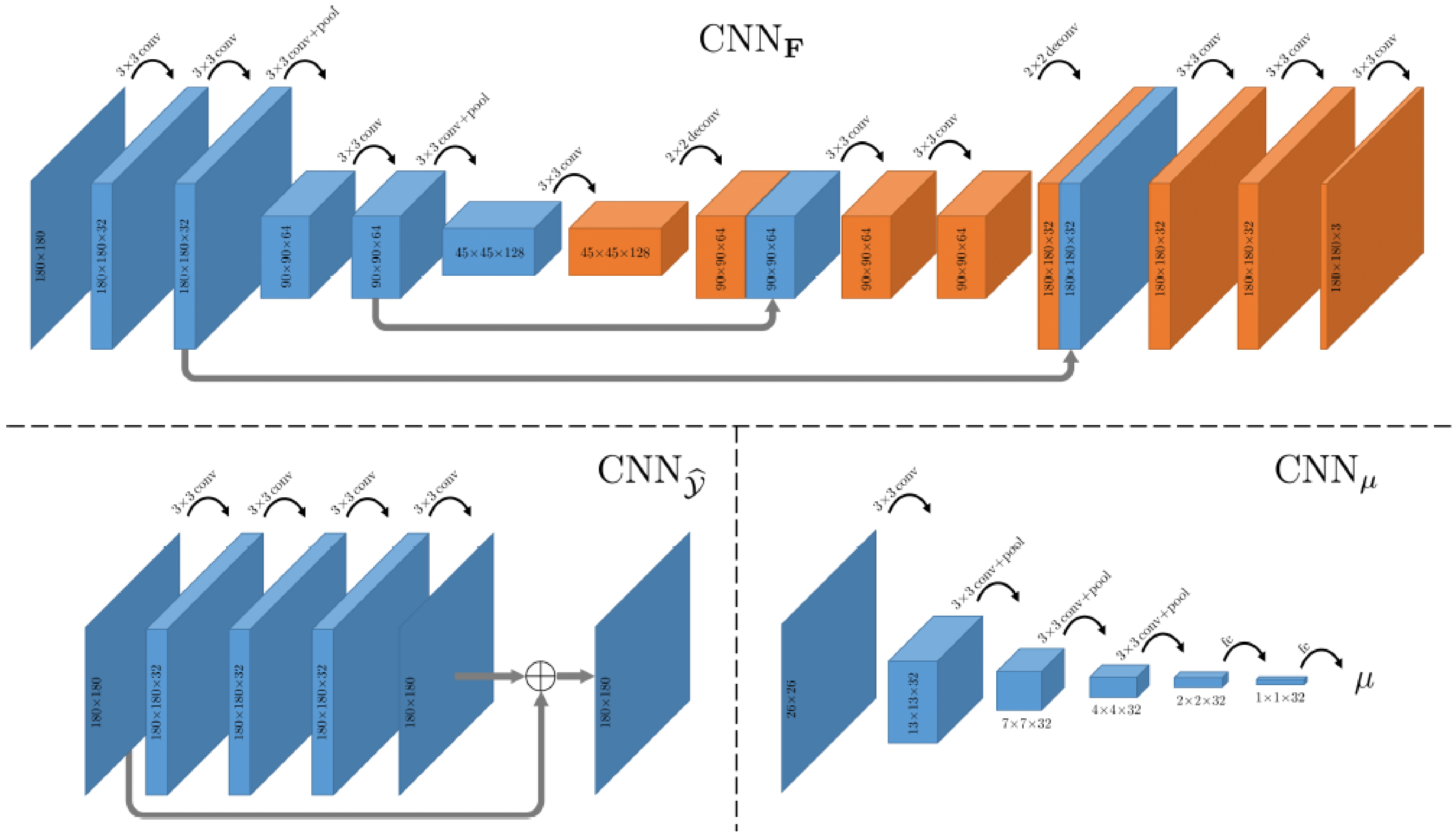

Fig. 3. Network architectures of CNN$_{\mathbf{F}}$, CNN$_{\widehat{\mathcal{Y}}}$ and CNN$_{\mu}$ in the experiments. Data produced by the decoder of CNN$_{\mathbf{F}}$ is colored in orange.

[1] J. Zeng et al., "**Deep Graph Laplacian Regularization**," submitted to arXiv, July 2018. (https://arxiv.org/abs/1807.11637)

Unrolling Graph Laplacian Regularizer

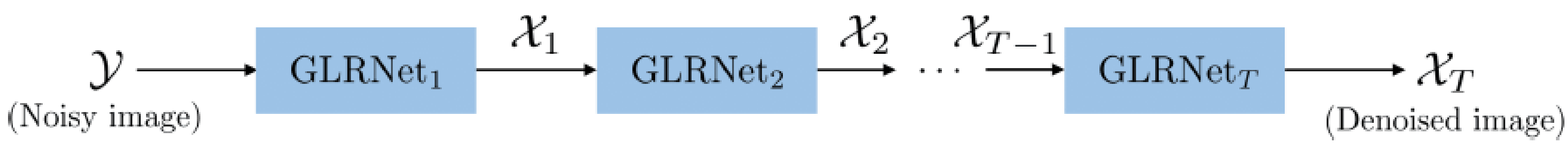

Fig. 2. Block diagram of the overall DeepGLR framework.

- **Graph Model** *guarantees numerical stability of solution*:

$$(\mathrm{I} + \mu \mathrm{L})\, \mathrm{x}^* = \mathrm{y}$$

- **Thm 1**: condition number κ of matrix satisfies [1]:

maximum node degree

$$\kappa \leq 1 + 2\,\mu\, d_{\max},$$

- **Observation**: By restricting search space of CNN to degree-bounded graphs, we achieve robust learning.

[1] J. Zeng et al., "**Deep Graph Laplacian Regularization**," submitted to arXiv, July 2018. (https://arxiv.org/abs/1807.11637)

Experimental Results – Numerical Comparison

- Trained on AWGN on 5 images, patches of size 26-by-26.
- Batch size is 4, model is trained for 200 epochs.
- Trained for both known and blind noise variance.

Table 1. Average PSNR (dB) and SSIM values of different methods for Gaussian noise removal. The best results for each metric is highlighted in boldface.

Noise	Metric	Method						
		BM3D	WNNM	OGLR	DnCNN-S	DnCNN-B	DeepGLR-S	DeepGLR-B
25	PSNR	29.95	30.28	29.78	**30.41**	30.33	30.26	30.21
	SSIM	0.8496	0.8554	0.8463	**0.8609**	0.8594	0.8599	0.8557
40	PSNR	27.62	28.08	27.68	28.10	28.13	**28.16**	28.04
	SSIM	0.7920	0.8018	0.7949	0.8080	0.8091	**0.8125**	0.8063
50	PSNR	26.69	27.08	26.58	27.15	27.18	**27.25**	27.12
	SSIM	0.7651	0.7769	0.7539	0.7809	0.7811	**0.7852**	0.7807

[1] Kai Zhang et al, "Beyond a Gaussian denoiser: Residual learning of deep CNN for image denoising," *TIP* 2017.
[2] Marc Lebrun et al, "The noise clinic: a blind image denoising algorithm," *IPOL* 2015.

Experimental Results – Numerical Comparison

- DeepGLR has average PSNR of 0.34 dB higher than CDnCNN [1].
- Model-based provides robustness against overfitting.

Table 2. Evaluation of different methods for low-light image denoising. The best results for each metric, except for those tested on the training set, are highlighted in boldface.

Metric	Noisy	Method					
		CBM3D	MC-WNNM	CDnCNN (train)	CDnCNN	CDeepGLR (train)	CDeepGLR
PSNR	20.36	26.08	26.23	33.43	31.26	32.31	**31.60**
SSIM Y	0.5198	0.8698	0.8531	0.9138	0.8978	0.9013	**0.9028**
SSIM R	0.2270	0.6293	0.5746	0.8538	0.8218	0.8372	**0.8297**
SSIM G	0.4073	0.8252	0.7566	0.8979	0.8828	0.8840	**0.8854**
SSIM B	0.1823	0.5633	0.5570	0.8294	0.7812	0.8138	**0.7997**

[1] Kai Zhang et al, "Beyond a Gaussian denoiser: Residual learning of deep CNN for image denoising," *TIP* 2017.
[2] Marc Lebrun et al, "The noise clinic: a blind image denoising algorithm," *IPOL* 2015.

Experimental Results – Visual Comparison

- trained on Gaussian noise, tested on low-light images in (RENOIR).
- Competing methods: DnCNN [1], noise clinic [2].
- outperformed DnCNN by 5.52 dB, and noise clinic by 1.87 dB.

DnCNN

clinic

DeepGLR

[1] Kai Zhang et al, "Beyond a Gaussian denoiser: Residual learning of deep CNN for image denoising," *TIP* 2017.
[2] Marc Lebrun et al, "The noise clinic: a blind image denoising algorithm," *IPOL* 2015.

Experimental Results – Visual Comparison

- trained on Gaussian noise, tested on low-light images in (RENOIR).
- Competing methods: DnCNN [1], noise clinic [2].
- outperformed DnCNN by 5.52 dB, and noise clinic by 1.87 dB.

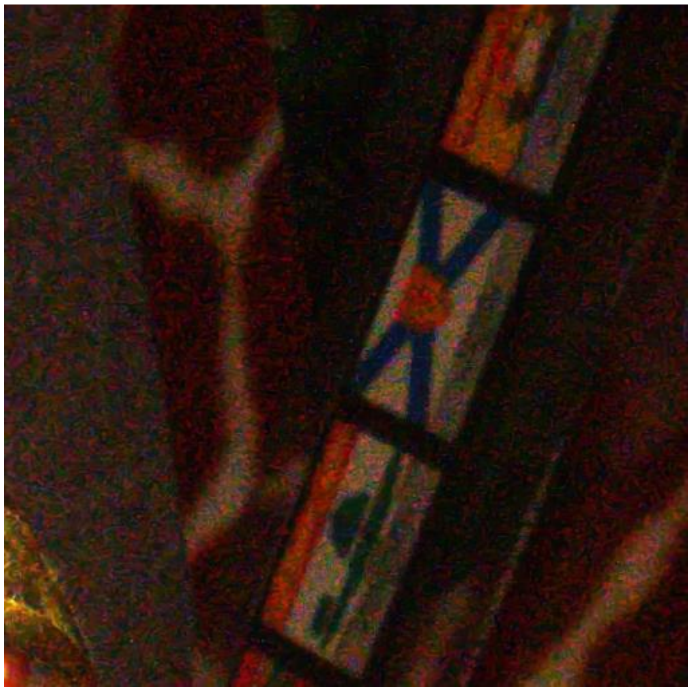

DnCNN

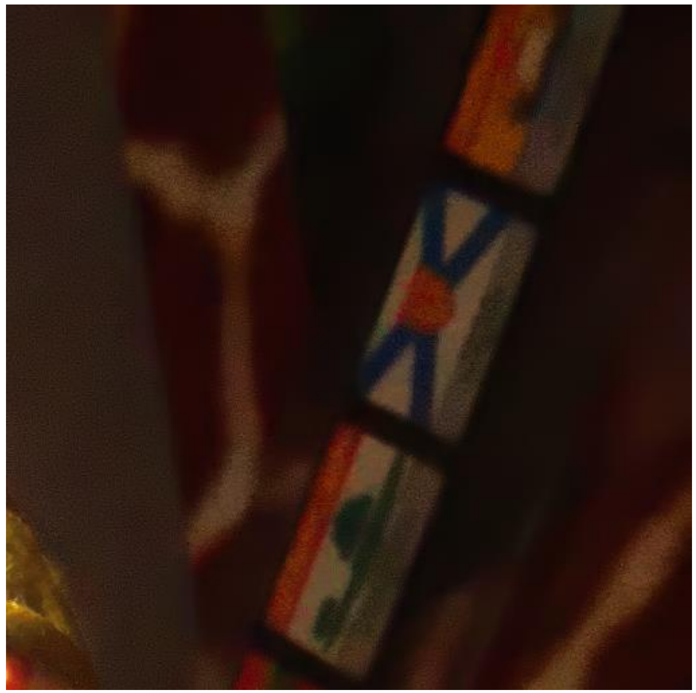

clinic

DeepGLR

[1] Kai Zhang et al, "Beyond a Gaussian denoiser: Residual learning of deep CNN for image denoising," *TIP* 2017.
[2] Marc Lebrun et al, "The noise clinic: a blind image denoising algorithm," *IPOL* 2015.

Experimental Results – Visual Comparison

- trained on Gaussian noise, tested on low-light images in (RENOIR).
- Competing methods: DnCNN [1], noise clinic [2].
- outperformed DnCNN by 5.52 dB, and noise clinic by 1.87 dB.

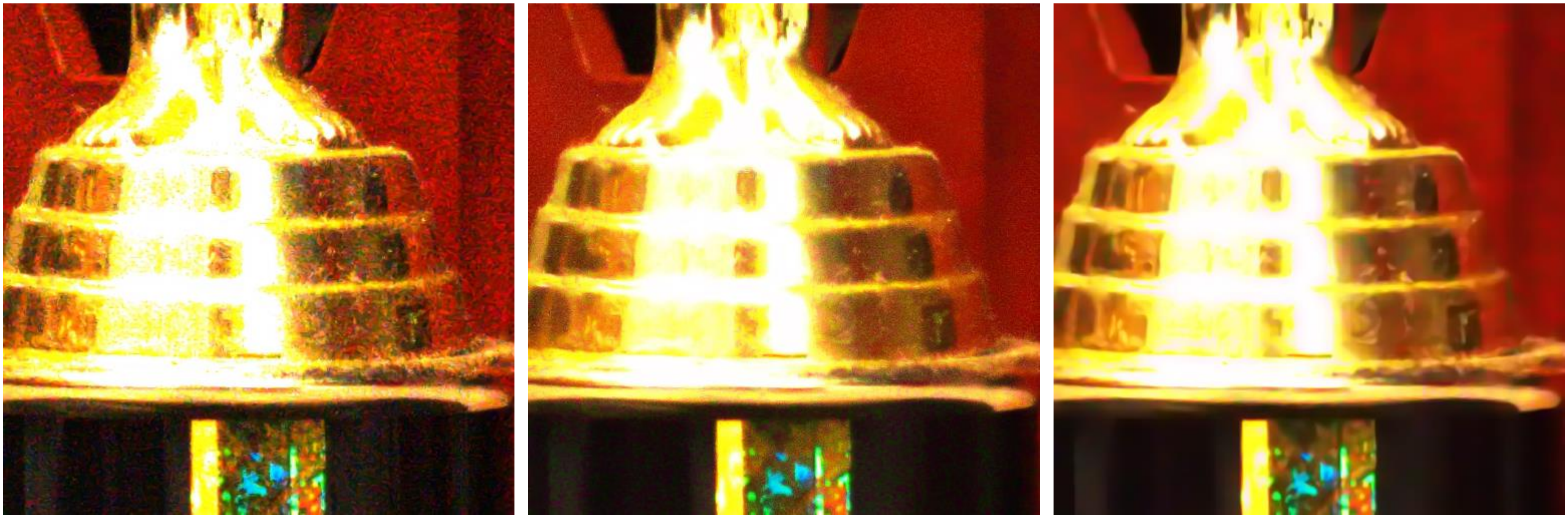

DnCNN clinic DeepGLR

[1] Kai Zhang et al, "Beyond a Gaussian denoiser: Residual learning of deep CNN for image denoising," *TIP* 2017.
[2] Marc Lebrun et al, "The noise clinic: a blind image denoising algorithm," *IPOL* 2015.

Outline

- GSP Fundamentals
- GSP for Image Compression
  - Optimality of GFT
- GSP for Inverse Imaging
  - Graph Laplacian Regularizer
  - Reweighted Graph TV: 3D Point Cloud Denoising
- Deep GLR
- Ongoing & Future Work

Summary

- Variants of GFTs for optimal decorrelation
  - GFT, GGFT, SGFT
  - Selection of statistical model vs. encoding cost of side information
- GSP for Inverse Imaging
  - PWS-promoting Graph Laplacian Regularizer, RGTV
  - Spectral interpretation of GTV, RGTV
- Graph-based model restricts search space of DNN.
  - Robustness against overfitting.

Ongoing & Future Work

- Unrolling of graph-based convex optimization.
  - Unrolling of ADMM, proximal gradient with GTV prior, convex set constraints.
  - Learn (sparse) connectivity, edge weights.
  - Learn features from RGBD images for depth inpainting / denoising.

- Model-guided learning safeguard against worst-case / adversary noise?

Q&A

- Email: genec@yorku.ca
- Homepage: https://www.eecs.yorku.ca/~genec/index.html